

## Chapter 6

### Modeling Io's Corona

#### 6.1 Introduction

In Chapter 3 I presented mutual event observations of Io's sodium corona. From these observations I determined the average state of the corona which is formed from the escape of Io's surface atmosphere. It also provides the source for the extended neutral clouds and the plasma torus. Therefore the corona provides a unique link between the the atmosphere and the large scale escape features. To understand the formation of the neutral clouds and the plasma torus it is essential that the processes which create and shape the corona are understood. The key to understanding the relationship between the loss from Io's atmosphere and the creation of the plasma torus is found in the corona. The discovery of a previously undetected asymmetry between the inner and outer hemispheres of the corona points to previously unknown processes at work close to Io's surface which affect the rate at which Io's atmosphere is stripped away and highlights the need for continued study of this region.

The previous chapter described the neutral cloud model which I have helped to develop so that the processes molding the corona can be determined and their implications for Io's atmosphere understood. This chapter applies the model from Chapter 5 to understanding the observations from Chapter 3. I also discuss recent *Hubble Space Telescope* observations of Io's oxygen corona (Roesler et al. 1999; Wolven et al. 2001) which point out several key differences between sodium and oxygen within  $6 R_{Io}$  of Io.

I use the neutral cloud model to interpret observational differences between the oxygen and sodium coronae.

The goals for this chapter are:

- (1) Determine the characteristics of the flux distribution of the neutrals escaping from Io's exobase.
- (2) Understand how deviation from the average plasma conditions affects the shape of the corona.
- (3) Study the implications of the observed corona asymmetry on loss from Io's exobase.
- (4) Compare the measured shapes of the oxygen and sodium coronae and determine implications for the sources of each.

In Section 6.2 I discuss the application of the model to the corona and describe the method of comparing the model to observations. Section 6.3 contains the model analysis of flux distributions from Io's exobase which can simulate the average observed corona and discuss how deviation from these flux distributions change the coronal shape. I also describe how the east/west electric field across the inner Jovian system creates the observed east/west sodium brightness asymmetry. The section concludes with an analysis of the effects of uniform variations affecting the entire torus and the observed periodic variations. The implications of the column density asymmetry between Io's inner and outer hemispheres on the spatial distribution of the loss from Io's exobase is described in Section 6.4. I conclude the chapter with a description oxygen corona based on the *HST* observations and the differences between the shapes of the sodium and oxygen coronae, discussing the implications of these differences on the loss from the exobase.

These studies can be combined with future observations of coronal variability to

determine the limits of variability in the torus and to probe the interaction between Io and the surrounding plasma. The coronal asymmetries, variations in the shape of the corona, and the differences between Io’s sodium and oxygen coronae are indicative of spatial and temporal anisotropies in the plasma torus and the loss of neutrals from Io’s exobase. A major focus of this chapter is understanding what produces variations in the shape of the corona allowing interpretation of future observations of these changes.

## 6.2 Description and Analysis of Model Runs

The mutual event observations discussed in Chapter 3 show that the column density profile in the corona can be described as a power law in the form:

$$N = N_0 b^{-s} \tag{6.1}$$

where  $b$  is the impact parameter in Io radii,  $N_0$  is the column density extended to Io’s surface, and  $s$  is the power law index. On log-log axes, this relation is linear with y-intercept =  $\log(N_0)$  and slope equal to  $(-s)$ . I will here use the terms “slope” and “power law index” interchangeably to refer to the quantity  $(-s)$ . When the slope is large, the corona is “steep;” a small slope implies a “shallow” corona.

For the corona models discussed, packets were evenly distributed over Io’s exobase (assumed to be  $1.4 R_{Io}$ ) and ejected isotropically from each point on the sphere surrounding Io with a specified flux speed distribution. The total time of each simulation was 20 hours with packets released at random times throughout the simulation. This duration was chosen such that all neutrals ejected at the beginning of the interval are lost (either by escaping Io, hitting Io’s surface, or ionization) by the end of the simulation. Model images of column density were produced and the radial column density profiles were computed from the positions and un-ionized fractions of the packets remaining at the end of the simulation (Figure 6.1). Power laws functions were fit to these profiles as functions of impact parameter to determine the slopes of the coronae produced with the

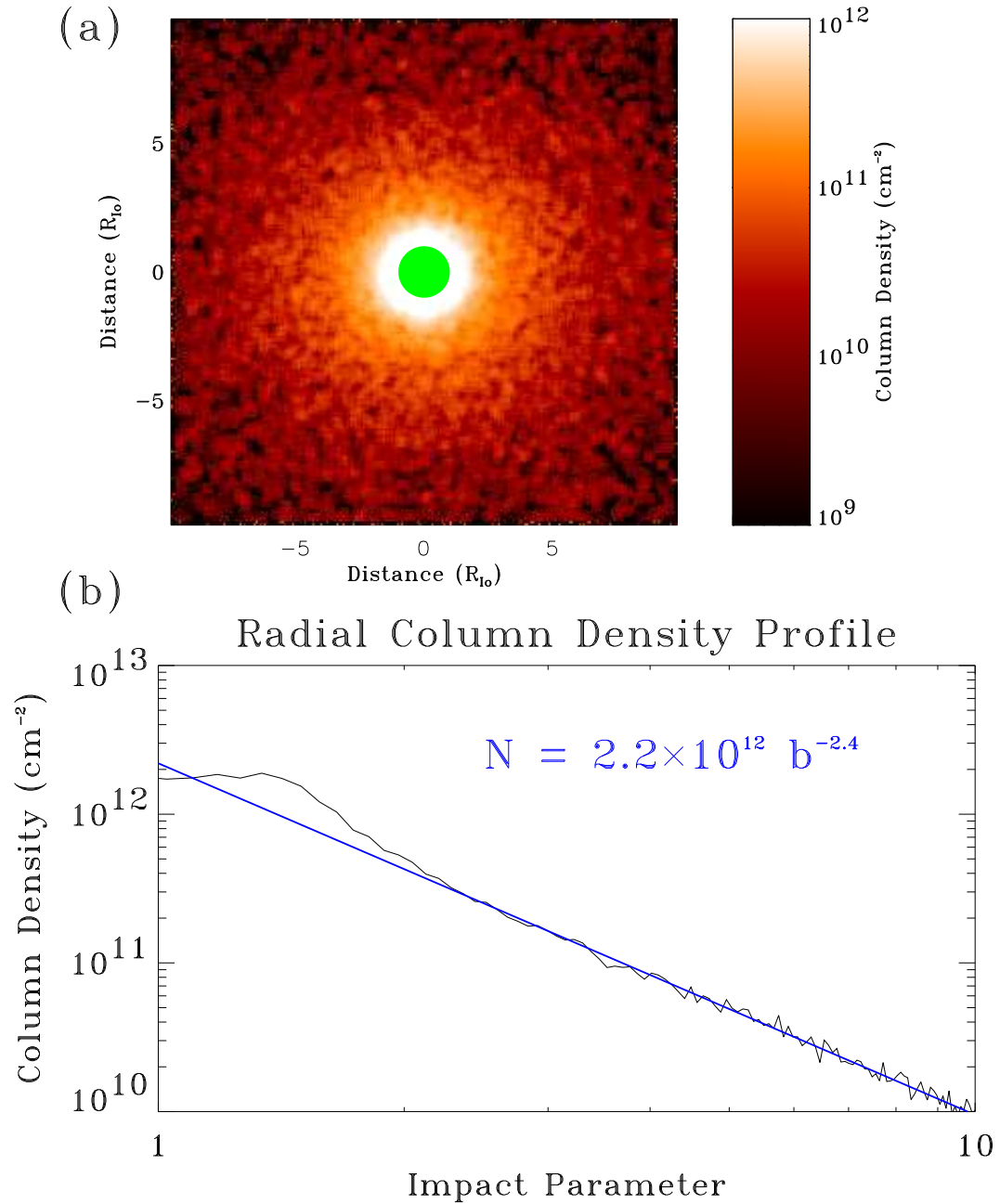


Figure 6.1 (a) Model image of the corona. Scale is logarithmic as indicated by the color scale bar. The image has been scaled such that the column density  $1 R_{\text{Io}}$  from the center is consistent with the mutual event observations (Equation 3.5). The green circle of radius  $1 R_{\text{Io}}$  represents Io's disk. (b) Radially averaged column density profile of the model image in (a) with best fit power law over-plotted in blue. Note that because the velocity distribution is truncated below  $0.75 \text{ km s}^{-1}$ , the radial profile does not accurately reflect the corona within  $\sim 2 R_{\text{Io}}$ .

specified parameters. To save computation time and memory, the speed distributions were truncated below  $v = 0.75 \text{ km s}^{-1}$  since packets below that speed do not make it far enough into the corona to affect the column density and could safely be ignored. Outside  $\sim 6 R_{\text{Io}}$ , Jupiter's gravitational pull begins to dominate over Io's. To avoid artifacts associated with the inner and outer edges, the power laws were fit to the radial profiles between  $b=2 R_{\text{Io}}$  and  $6 R_{\text{Io}}$ , which also corresponds to the regions with the highest quality mutual event data.

### 6.3 Understanding the Shape of the Corona

The mutual events discussed in Chapter 3 describe a radially averaged corona with the shape:

$$N(b) = 2.2_{-0.7}^{+1.4} \times 10^{12} b^{-2.34_{-0.34}^{+0.27}} \text{ cm}^{-2} \quad (6.2)$$

If sodium escaped freely without ionization or the influence of Io's gravity, the column density in the corona would be proportional to  $b^{-1}$ . The significantly faster rate at which the observed corona column density decreases is due to the combined effects of Io's gravity, which slows the escaping atoms, and ionization in the corona. In this section I discuss how this average corona can be created when the velocity distribution of sodium escaping from the exobase can be described by either a sputtering or exponential distribution. I also examine how departure from these parameters affects the corona and look for changes in its shape with orbital phase and magnetic longitude.

#### 6.3.1 The Average Observed Corona

It is possible to adequately model the corona using a range of source distributions, even when using the basic torus model that does not include any System-III variability. Figures 6.2 and 6.3 show how the shape of the corona and the source rate vary with changes in the source flux distribution. The average state of the corona can be modeled using either the sputtering distribution (Equation 2.12) or the exponential distribution

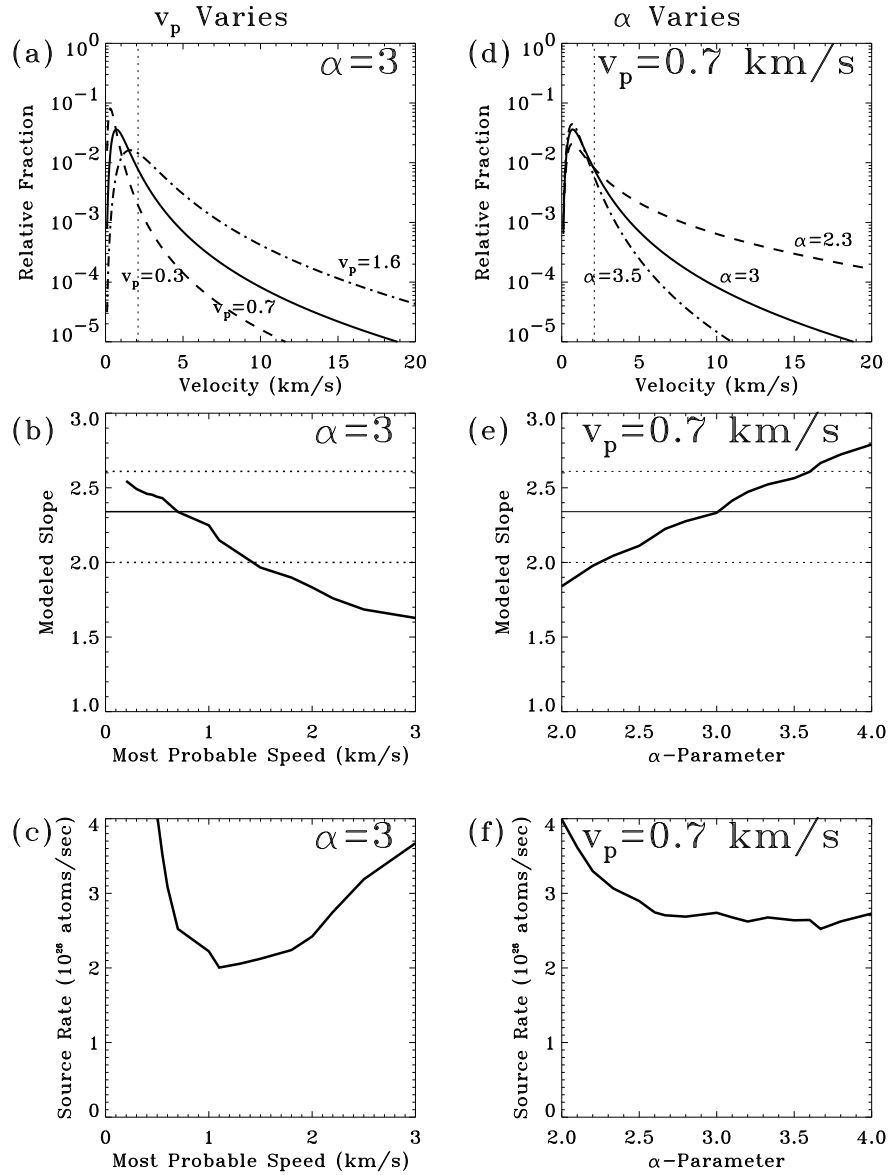


Figure 6.2 Radially averaged models of the observed average sodium corona. (a) Flux distributions at the speeds required to approximate the variability in the corona for the true sputtering case. The dotted line at  $v = 2.1$  km s $^{-1}$  indicates escape velocity from Io's exobase. (b) Modeled corona slope using a pure sputtering corona ( $\alpha = 3$ ) and varying the most probable speed of the distribution. The solid horizontal line shows the average observed slope; the broken lines show the  $1-\sigma$  variation. (c) Source rate needed to match the observed (extrapolated) surface column density of  $2.2 \times 10^{12}$  cm $^{-2}$ . (d) Sputtering distributions with the most probable speed held constant and  $\alpha$  varied as indicated. (e) Modeled corona slope holding the most probable speed constant at  $0.7$  km s $^{-1}$  and varying the  $\alpha$ -parameter. (f) Modeled source rate for models with  $v_p = 0.7$  km s $^{-1}$  as function of  $\alpha$ .

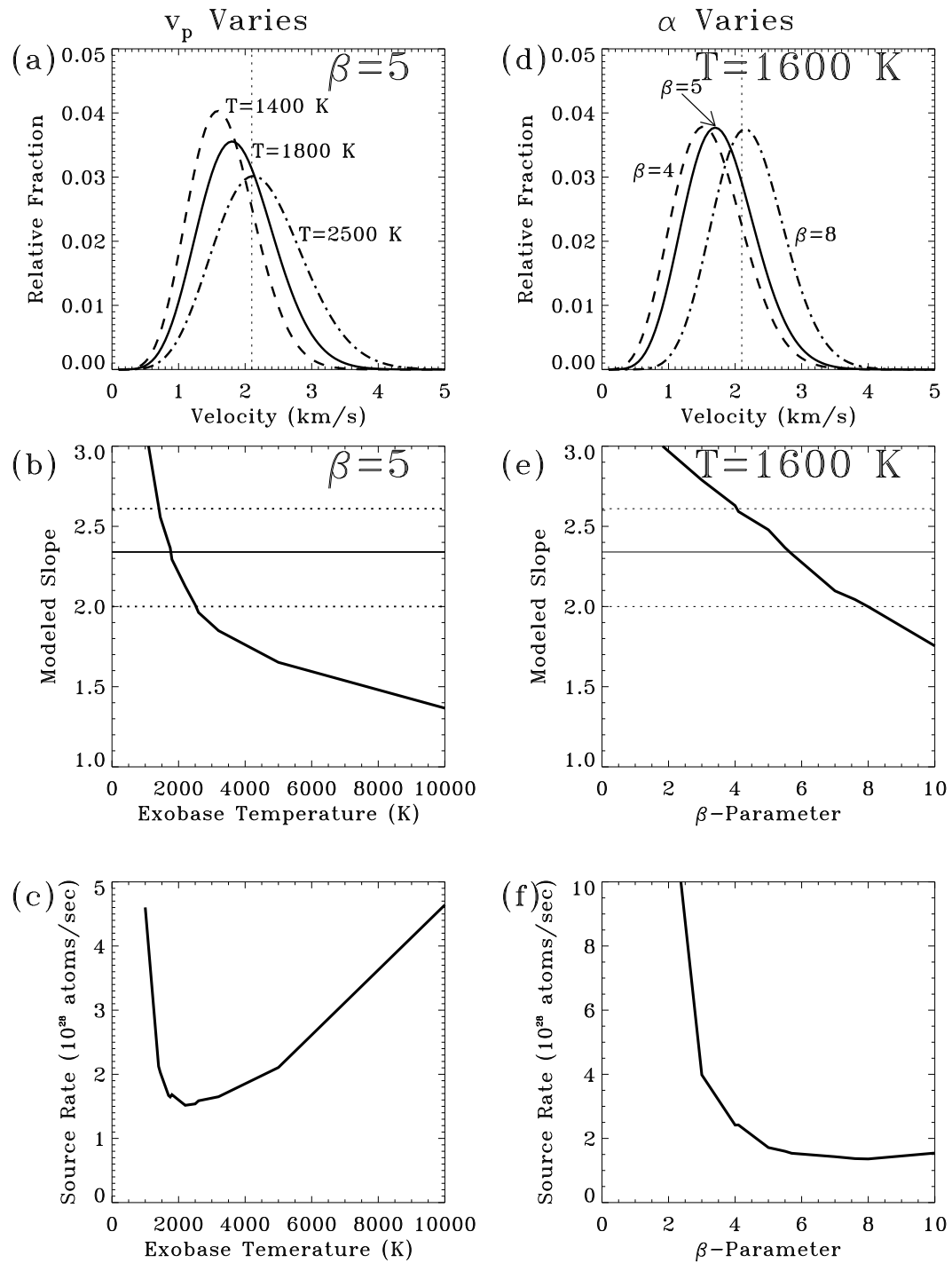


Figure 6.3 Same as Figure 6.2 using a exponential source distribution. In the left panels, the exobase temperature is varied while holding  $\beta = 5$  constant, corresponding to a Maxwell-Boltzmann distribution for the escaping sodium. In the right panels, the temperature is held constant while the  $\beta$ -parameter varies.

(Equation 5.16), as discussed below. The torus model used to determine the sodium lifetime for the models in Figures 6.2 and 6.3 is the Basic Torus which does not vary with magnetic longitude. The effects of departures from this torus and of magnetic longitude variations in the torus are examined in the following sections.

The sputtering distribution, as can be seen in Figure 6.2, can create a corona similar to the average corona for a wide variety of parameter choices. The best fit for a pure sputtering distribution ( $\alpha = 3$ ) is with a most probable velocity  $v_p \sim 0.7 \text{ km s}^{-1}$  and a source rate of  $2.7 \times 10^{26} \text{ atoms s}^{-1}$ , somewhat higher than previous results. The slope in the actual corona was found to vary between 2.0 and 2.6. As the most probable speed decreases, the corona becomes steeper. Using the pure sputtering distribution and the average torus conditions, the most probable speed would need to be less than  $0.3 \text{ km s}^{-1}$  for the corona to drop off as quickly as  $b^{-2.6}$ . The lower bound of the slope can be achieved by increasing the most probable speed to  $1.6 \text{ km s}^{-1}$ .

The importance of higher speed sodium on the shape of the corona is examined by varying the  $\alpha$ -parameter while holding the most probable speed constant. Decreasing the value of  $\alpha$  increases the relative amount of sodium with escape velocity. Figure 6.2(b) shows that varying  $\alpha$  between 2.3 and 3.5 captures the full range of variability in the observed slope of the corona. However, these values of  $\alpha$  do not actually have any physical significance and should only be viewed as an example of how the speed distribution needs to vary to model the corona, and not as an exact description of escape from Io's exobase.

The right panels of Figure 6.2 show the source rate required to match the observed value of  $N_0 = 2.2 \times 10^{12} \text{ cm}^{-2}$  in Equation 6.2, which is the column density of sodium extrapolated to the surface assuming the power law in the corona extends all the way down. The value of  $N_0$  is directly proportional to the source rate so variability in this value unaccompanied by variation in the slope can be interpreted as variations in the rate of neutral sodium atoms escaping from the exobase.

	$v=0.5 \text{ km s}^{-1}$ $\alpha = 7/3$	$v=0.7 \text{ km s}^{-1}$ $\alpha = 3$	$v=1.0 \text{ km s}^{-1}$ $\alpha = 3$
<b>Old <math>\sigma</math></b>	$8.1 \times 10^{11} b^{-2.3}$	$1.2 \times 10^{12} b^{-2.7}$	$1.4 \times 10^{12} b^{-2.5}$
<b>Radial Ejection</b>	$2.0 \times 10^{12} b^{-2.5}$		$1.5 \times 10^{12} b^{-2.5}$
<b>New <math>\sigma</math></b>	$7.7 \times 10^{11} b^{-2.1}$	$1.2 \times 10^{12} b^{-2.5}$	$1.5 \times 10^{12} b^{-2.3}$
<b>Radial Ejection</b>			
<b>Old <math>\sigma</math></b>	$5.6 \times 10^{11} b^{-2.1}$	$8.5 \times 10^{11} b^{-2.6}$	$1.0 \times 10^{12} b^{-2.3}$
<b>Isotropic Ejection</b>			
<b>New <math>\sigma</math></b>	$6.3 \times 10^{11} b^{-2.0}$	$8.2 \times 10^{11} b^{-2.3}$	$1.1 \times 10^{12} b^{-2.2}$
<b>Isotropic Ejection</b>			

Table 6.1 Comparison of corona created with different cross sections and different ejection direction distributions. The corona profiles modeled by Smyth and Combi (1988b) are shown in boxes where available. Power law results are the average corona profile assuming a total exobase source rate of  $10^{26}$  atoms  $s^{-1}$ .

This average result is similar to that of Smyth and Combi (1997) who determined that an exobase source rate of  $1.3 \times 10^{26}$  atoms  $s^{-1}$  for the pure sputtering case with a most probable speed of  $1.0 \text{ km s}^{-1}$ . These authors preferred  $\alpha = 7/3$  because it produced more fast sodium that they believed was needed to explain Io's fast sodium features. Using this value, they found a most probable speed of  $0.5 \text{ km s}^{-1}$  and exobase source rate of  $1.7 \times 10^{26}$  atoms  $s^{-1}$  for this distribution. There are several differences between the current work and the previous results which may help to explain the different results. First, as discussed in Chapter 5, this model uses different sodium electron impact cross sections and a different parameterization of the plasma torus. Second, Smyth and Combi used the mutual event results of Schneider et al. (1991a) which described a somewhat steeper corona with an average slope of  $\sim 2.5$ . Lastly, they assumed that the sodium was all ejected radially from Io's exobase while this work uses an isotropic directional distribution.

Table 6.1 contains a comparison of the different coronae created with the two published cross sections and the corona created with isotropic or radial ejection. Several basic conclusions can be drawn from this the corona profiles listed. First, the old cross section, which predicts a shorter sodium lifetime, results in a steeper corona. This is

because more sodium atoms make it to the outer reaches of the corona when the lifetime is longer, creating a shallow, more extended corona. The dynamics of the atoms' motions are the same, but the change in lifetime changes the shape of the corona. Second, isotropic ejection creates a shallower corona than radial ejection. Isotropic ejection has two effects on the distribution of neutral atoms. First, atoms ejected tangentially to the surface with velocities near the escape speed stay in the corona longer than atoms ejected perpendicular to the surface, since these atoms are more likely to orbit Io before impacting the surface or being ionized. Second, atoms ejected from any point on the exobase can contribute to any part of the corona. This reduces the effects of variations in the spatial distribution of the sputtering. The actual directional distribution is most likely some intermediate between purely radial and purely isotropic ejection. Neutrals can be sputtered in all directions, but the distribution is more concentrated radially outward than tangential to the surface.

The average corona is also well matched using the exponential distribution with  $\beta = 5$ , corresponding to a Maxwell-Boltzmann speed distribution, with a temperature of  $\sim 1800$  K and an exobase escape rate of  $1.8 \times 10^{28}$  atoms  $\text{sec}^{-1}$ , which is about two orders of magnitude greater than the estimate for the source rate of sputtered sodium. This is due to the fact that there is very little high speed sodium in this distribution and therefore the source rate must be extremely high to populate the outer regions of the corona. The observed variability in the corona is modeled by varying the temperature between 1400 K and 2500 K. These temperatures are consistent with both the measurements of the coronal temperature ( $\sim 1600$  K from Chapter 3) and model estimates for the temperature of the exobase ranging from 200 K to 3000 K (Wong and Smyth 2000).

I have also looked at how changing the shape of the exponential distribution affects the shape of the corona by changing the  $\beta$ -parameter while keeping the temperature constant. For a 1600 K exobase, the observed variation can result from varying

$\beta$  between 4 and 8. As for the similar exercise discussed above for the sputtering distribution, this does not necessarily have any physical significance but indicates that a significant fraction of the sputtered sodium must have escape velocity to populate the outer regions of the corona.

Apart from reproducing the observed corona, it is instructive to look at how changes in the source distribution affect the shape of the corona. The general trend is that anything which increases the amount of sodium with escape velocity relative to slower, non-escaping sodium, creates a “flatter” corona which extends further from Io. Speed distributions which contain a high percentage of non-escaping sodium create coronae which stay close to Io. This tendency is explained by the fact that little sodium leaving the exobase with escape velocity is ionized before it can escape the corona. Slower sodium, even if it has sufficient velocity to make it to the outer regions of the corona, takes longer to travel that far and is more likely to be ionized and fail to contribute to the neutral component. Sodium leaving the exobase at  $3 \text{ km s}^{-1}$  takes only 0.9 hours to make it to  $6 R_{\text{Io}}$ , as opposed to the 2.2 hours it takes for sodium traveling at  $2 \text{ km s}^{-1}$ . Assuming an approximate lifetime of 4 hours for sodium, 80% of the faster moving sodium survives compared with 58% of the slower sodium (Figure 6.4).

Another interesting result shown in Figures 6.2(e) and 6.3(e) is that the the source rate necessary to match the observations increases for very small and very large most probable velocities. When the most probable speed of the distribution is small, a large fraction of the sodium immediately returns to Io; only the tail end of the distribution is making it into the corona. Therefore the source rate needs to be pumped up to produce the amount of sodium necessary to match the observed  $N_0$ . Since it is only the high speed tail of the distribution which contributes to the density near the exobase, very little sodium makes it farther out into the corona and corona drops off very quickly, creating a corona with a large slope. For speed distributions with higher most probable

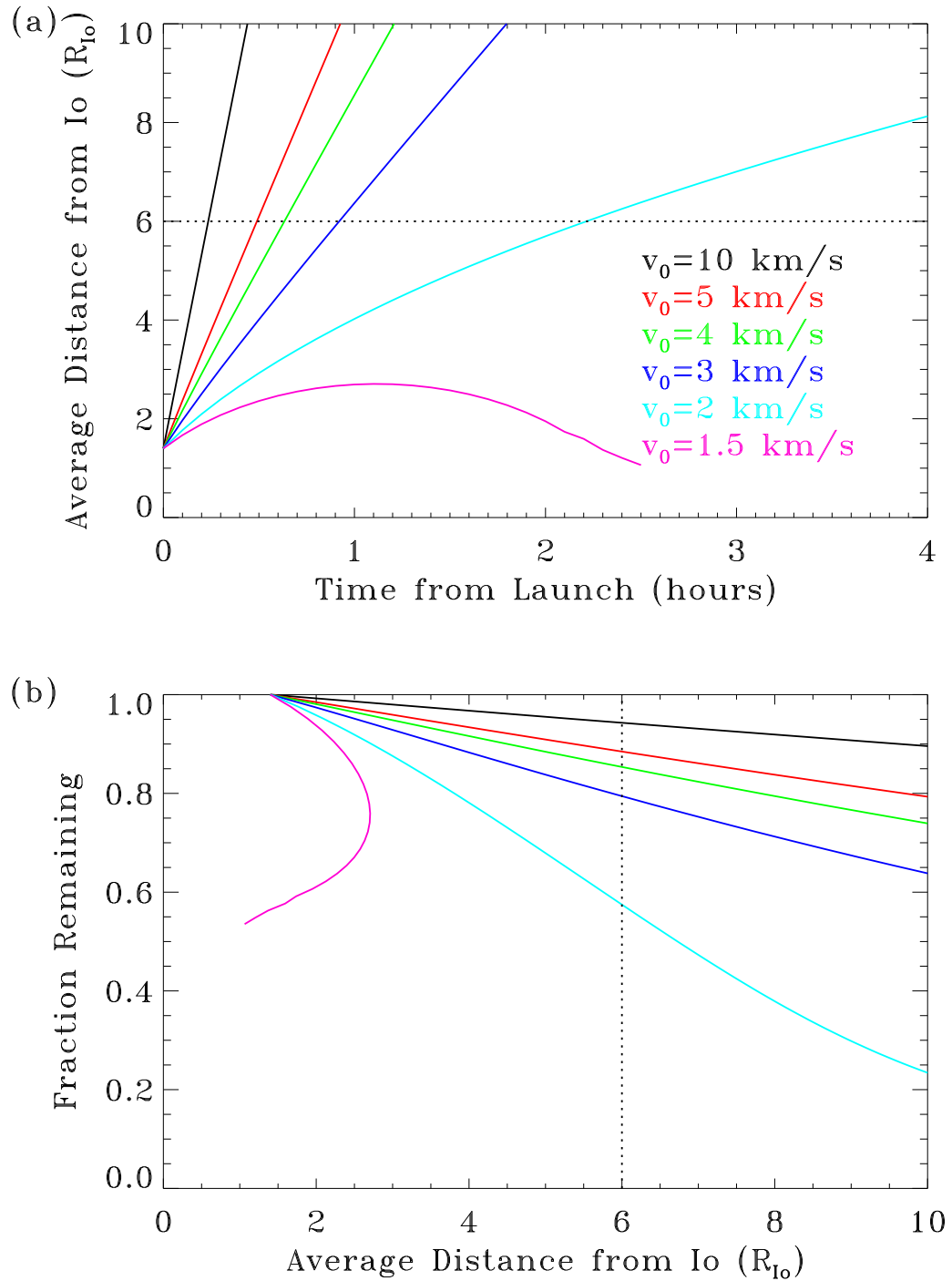


Figure 6.4 (a) Distance from Io of sodium atoms versus time since launch from the exobase. The initial velocity of the atoms is indicated. The dotted at  $r=6R_{Io}$  indicates the approximate location of the Hill sphere which corresponds to the outer edge of the corona. (b) Un-ionized sodium fraction versus distance from Io for atoms with the specified initial velocity assuming a constant 4 hour lifetime.

speeds, the source rate increases because less sodium stays near the exobase: the flux through the exobase is high, decreasing the density near Io. The source rate must be increased to offset the effects of the high flux.

### 6.3.2 Variations in the Average Corona

Variations in the plasma environment at Io affect the lifetime of neutrals in the corona. These variations can be grouped into several categories. First, Jupiter's offset tilted dipole means that the plasma density at Io varies with a period of approximately 10 hours with the electron density being greatest when Io crosses the centrifugal equator ( $\lambda_{Io} = 110^\circ$  and  $290^\circ$ ). When Io is north or south of the torus, the electron density is lower and the sodium lifetime is greater. Since the time-span between maximum and minimum lifetimes is comparable to the amount of time a neutral sodium atom remains in the corona ( $\sim 2$  hours), variations in the corona due simply to the dipole are expected to be small.

The east/west electric field across the Jovian system results in variations with orbital phase in the plasma at Io in two ways: First, the torus is offset from the center of the dipole by an amount proportional to the strength of the electric field, meaning that Io's position relative to the cold torus, ribbon, and warm torus change with Io's orbital phase. Second, as the plasma is swept around Jupiter from west to east, it expands, decreasing the density. This is responsible for the east/west brightness asymmetry near Io (Smyth and Combi (1988b) and see below).

The last type of variability is the observed System-III variability (e.g. Schneider and Trauger (1995)). This variation is treated as variability in the ion temperature, which changes the scale height of the torus and the electron density at the centrifugal equator. This increases both the average sodium lifetime at Io and the range of lifetimes in the corona.

In this section, I explore the effects of each of these three categories of variations

on the shape of the corona using the average sputtering parameters determined above ( $\alpha = 3$ ,  $v_p = 0.7 \text{ km s}^{-1}$ ) as a reference point. Orbital phase effects are measured by looking at the shape of Io's corona at four points in its orbit: when Io is behind Jupiter ( $\phi = 0^\circ$ ), at eastern elongation ( $\phi = 90^\circ$ ), in front of Jupiter ( $\phi = 180^\circ$ ), and at western elongation ( $\phi = 270^\circ$ ). The modeled slope (-s) and the intercept assuming a source rate of  $2.7 \times 10^{26} \text{ atoms s}^{-1}$  ( $N_0$ ) are used to provide a comparison to the observed corona.

### 6.3.3 Building to an Offset Tilted Dipole with an East/West Electric Field

Three steps were taken to work up to the basic torus described in Chapter 5. First I looked at the corona in a torus centered on Jupiter that is not tilted relative to Jupiter's equatorial plane. The lifetime at Io was a constant 3 hours when using the Voyager torus measurements. The slope remains constant in this case with the coronal column density proportional to  $b^{-2.4}$ .

A more interesting case is that with Jupiter's offset, tilted dipole, which causes the torus to be inclined relative to Jupiter's equatorial plane. Figure 6.5(a)-(c) shows the effect of the dipole on the sodium lifetime and corona. The shape of the corona was computed as functions of orbital phase and magnetic longitude. The lifetime in this case is constant with orbital phase, since the time-averaged torus has cylindrical symmetry about Jupiter's rotational axis, but varies with magnetic longitude due to both the tilt and offset of the dipole. As shown in panels (b) and (c), the effect of the true dipole is small: there is no appreciable dependence on either orbital phase or magnetic longitude on the shape of the corona. This is due to a combination of factors: first, when the torus is symmetric about Jupiter, the only effect which is asymmetric with respect to Io's orbital phase is radiation pressure, which is too small in magnitude to have any measurable consequences in the corona. Second, the range of lifetimes experienced by sodium atoms is small, diminishing the importance of the changing lifetime. Lastly, the

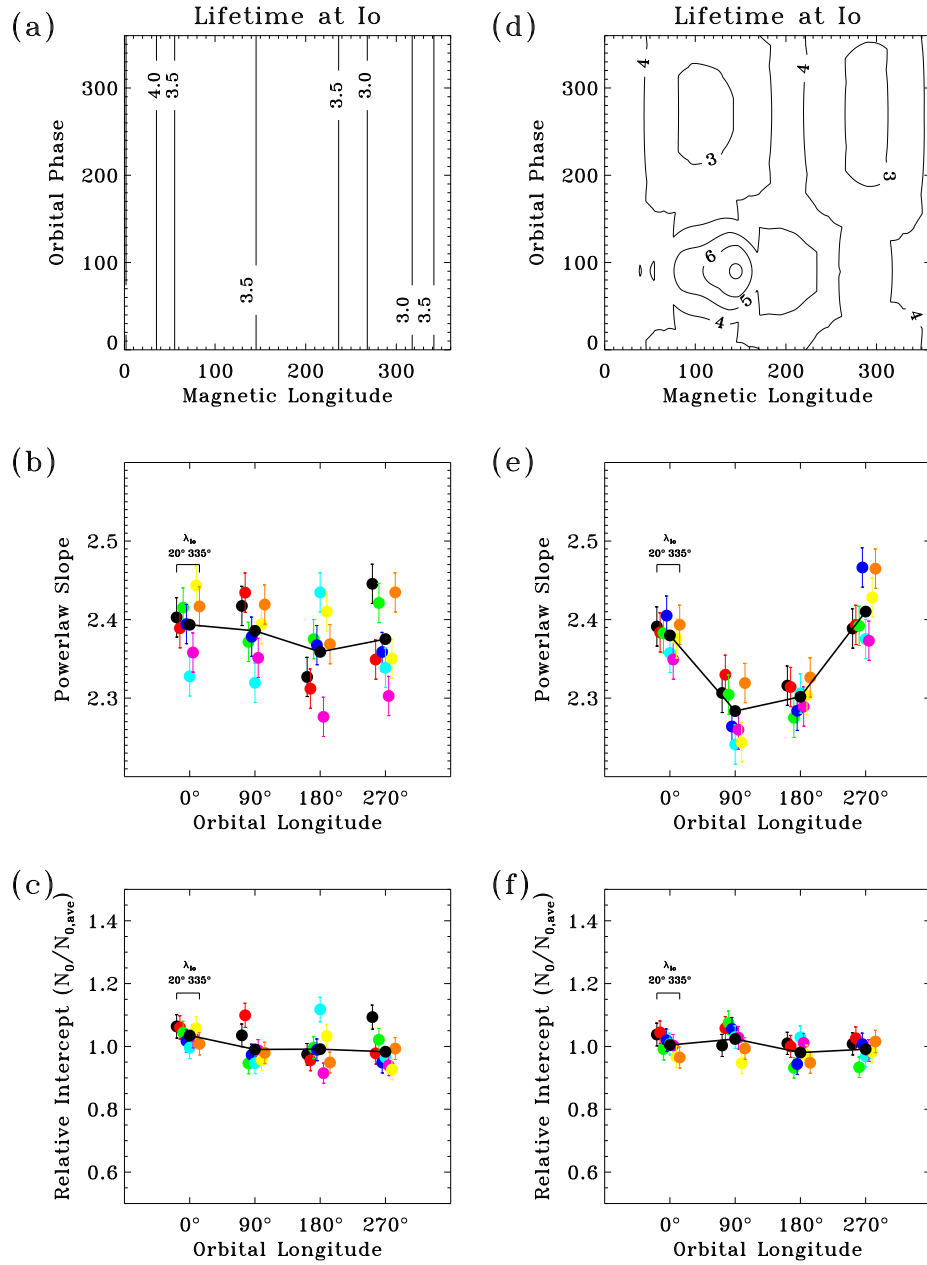


Figure 6.5 The effects of Jupiter’s offset tilted dipole and the east/west electric field on the power law fit to the modeled corona. In panels (a)-(c), Jupiter’s dipole is included, but the east/west electric field is turned off. In panels (d)-(f) the full offset tilted dipole with the inferred east/west electric field is used. Panels (a) and (d) show contours of the sodium lifetime at Io in hours as a function of the magnetic and orbital longitudes. Panels (b) and (e) show the best fit slope for the corona with uncertainties. Each clump of points shows models for Io at a single orbital location with the magnetic longitude increasing in each clump from left to right. Panels (c) and (f) give the modeled power law intercept relative to the average value of  $N_0 = 2.2 \times 10^{12} \text{ cm}^{-2}$ .

time scale for these changes is not much longer than the lifetime, so that the average state of the plasma which any individual atom is subjected to does not vary much with magnetic longitude.

The inclusion of the east/west electric field shifts the torus eastward by  $0.14 R_J$  at Io's orbit. The consequences of this shift are demonstrated in Figure 6.5(d)-(f). The electric field introduces a strong orbital phase asymmetry in the sodium lifetime which varies on a time scale significantly longer than the average lifetime (40 hours compared to  $\sim 4$  hours). Atoms ejected when Io is east of Jupiter make it farther from Io before ionization resulting in a more extended corona.

Interestingly enough, the intercept does not appear to vary significantly for this same torus implementation. This provides a demonstration of how the east/west electric field produces the local time asymmetry in the sodium cloud (Bergstralh et al. (1975, 1977) and see Section 5.4.2). As demonstrated by Smyth and Combi (1988b), the increase in sodium lifetime near eastern elongation results in increased sodium emission there compared to western elongation. These authors did not discuss how the electric field affects the shape of the corona. When the lifetime is longer, a larger fraction of the sodium sputtered from the exobase can make it to the furthest reaches of the corona before being ionized, thus decreasing the slope and increasing the total number of sodium atoms in the corona. The change in lifetime is sufficient to create the observed sodium brightness asymmetry (Figure 6.6). Without the electric field, the asymmetry disappears. In Figure 6.6, panel (a) shows the total column through the corona both with (blue squares) and without (red circles) the east/west electric field turned on. The total column was determined by creating a model column density image of the corona and totaling all the atoms in the annulus with impact parameter is between 2 and  $6 R_{Io}$  and averaged for all magnetic longitudes. The column density without the electric field remains constant with orbital phase; with the electric field, the column density is maximized at eastern elongation. The right panel shows the intensity in the

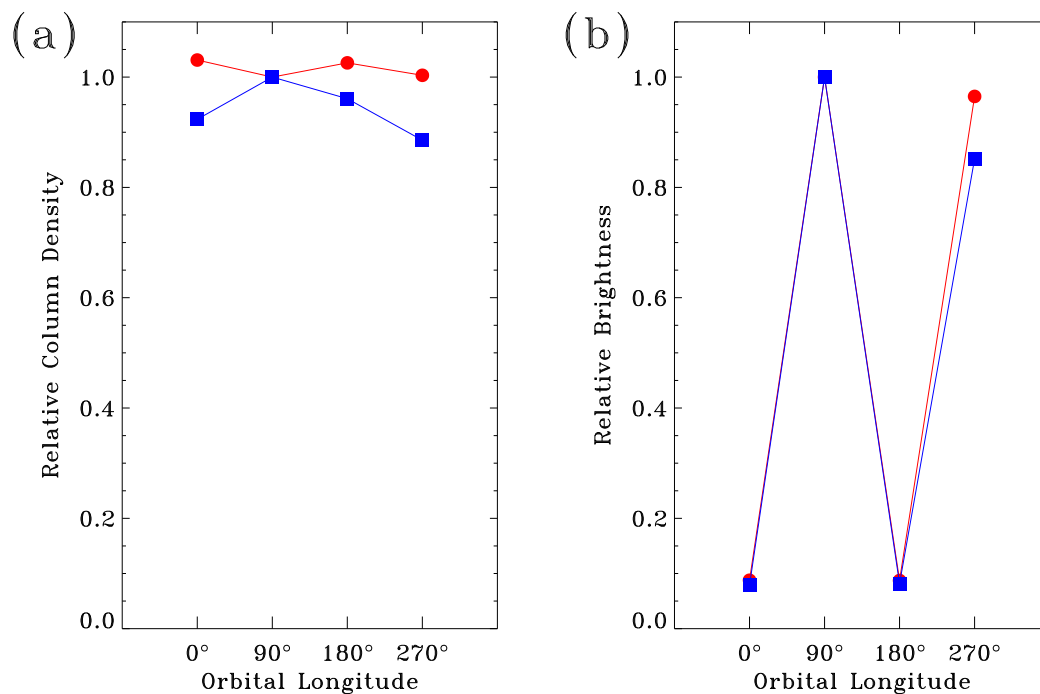


Figure 6.6 A demonstration of the effect of the east/west electric field on the sodium emission from the corona. (a) The total column of sodium atoms in the corona (impact parameter between 2 and 6  $R_{I_0}$  summed along the line of sight) with (blue squares) and without (red circles) the east/west electric field normalized to the value at eastern elongation. (b) Total intensity in the Bergstrahl slit with and without the electric field normalized to the intensity at eastern elongation.

slit of Bergstrahl et al. (1977) (8" by 3" aligned north/south across Io). As expected from the varying radial velocity relative to the sun, the intensity is a strong function of orbital phase (see Chapter 7 for a more complete discussion of this effect). However, the east/west ratio is not constant between the two cases, a consequence of the varying column density shown in the left panel. The east/west asymmetry seen in the case without the electric field is due to the slight asymmetry in the solar D<sub>2</sub> Fraunhofer line.

The mutual event observations cannot confirm or refute the changing shape of the corona between eastern and western elongation. Although no change in slope was detected, the predicted variation is smaller than the event to event fluctuations and only one event was observed near eastern elongation. In addition, this one event (Event #7, Table 3.1) was of lower than average quality. A better sampling of orbital phases is necessary to detect the expected variation in slope with local time.

#### 6.3.4 Effect of Uniform Variations in the Torus on the Corona

Another instructive experiment is to look at the effects of uniform variations in the plasma torus on the neutral clouds; i.e., variations which affect the entire torus in the same way. I discuss here three distinct types of changes in the torus structure: variations in the electron density, variations in the ion temperature, and variations in the inferred strength of the east/west electric field.

Electron density variations have a direct effect on the lifetime of the sodium near Io. Since the ionization rate due to electron impacts is proportional to  $n_e$  (Equation 2.14), the lifetime varies inversely with electron density: the lower the electron density, the denser and more extended the corona. Figure 6.7 shows how the shape of the corona varies when the electron density in the torus is uniformly modulated by constant factors of 1/2 and 2 compared to the Voyager measurements. The most prominent feature in the contour plots of sodium lifetime (top three panels) is that the lifetime is longest when the electron density is half that measured by Voyager and shortest when

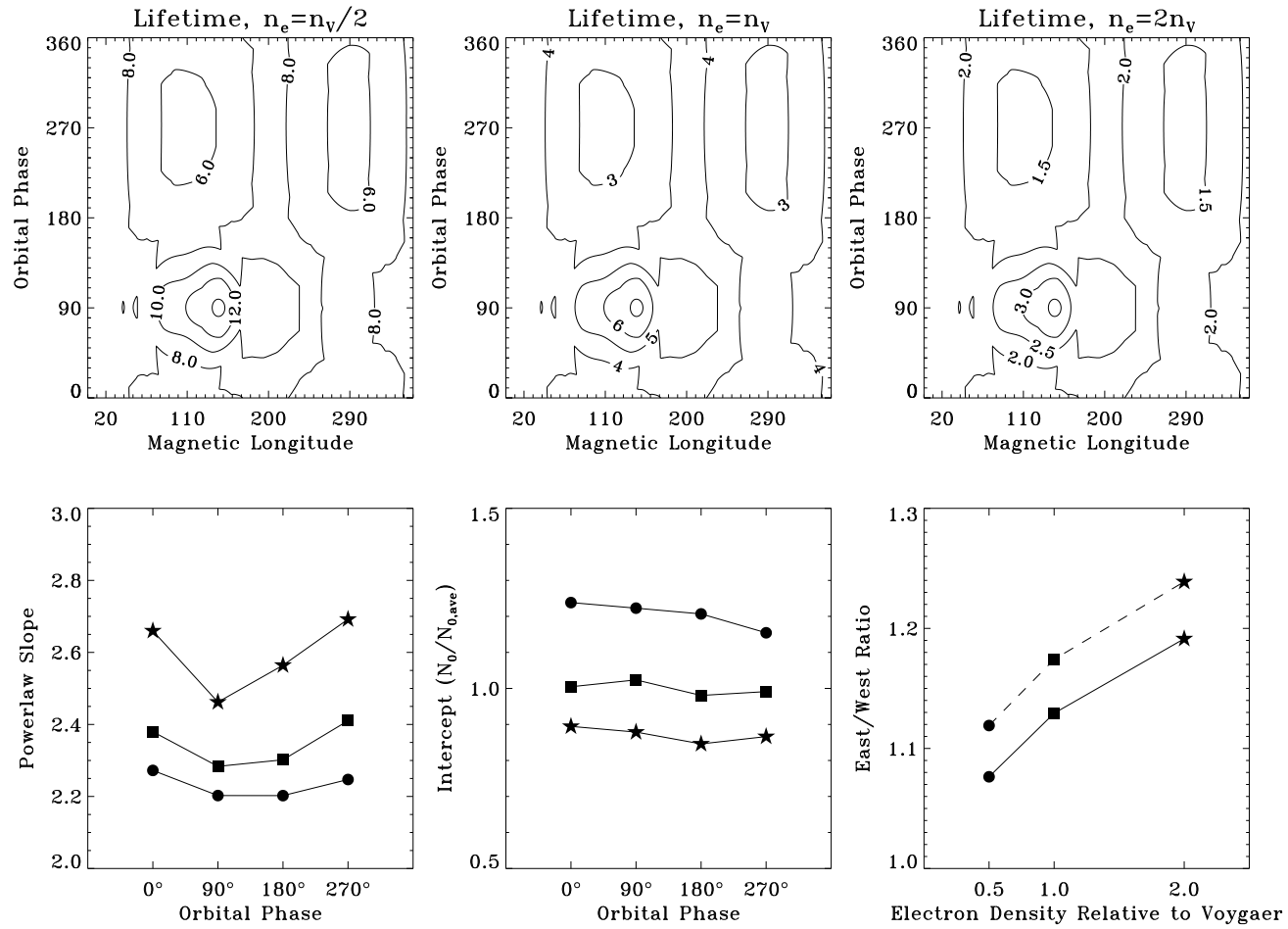


Figure 6.7 Effect of uniformly varying the electron density in the plasma torus on the sodium corona. The top three panels show contours of sodium lifetime at Io when the electron density is half, the same as, and twice that measured by Voyager ( $n_V$ ), respectively. The bottom left and middle panels give the power law slope and intercept for the three cases as a function of the orbital phase. The circles denote  $n_e = n_V/2$ , the squares denote  $n_e = n_V$ , and the stars show  $n_e = 2n_V$ . Panel (f) shows the modeled east/west density ratio (solid line) and east/west brightness ratio (broken line) for each case.

the electron density is twice the Voyager values. However, the morphology of these contour plots does not change between cases: Jupiter's dipole and the east/west electric field still produce the same effects.

The change in electron density produces large variations in the shape of the corona. As the electron density increases, the power law slope increases and the intercept decreases. The increasing slope implies that the corona is much less extended. The decreasing intercept means that more sodium must be ejected from the exobase to produce the observed  $N_0$ . These are both consequences of the short sodium lifetime: sodium is ionized close to the source so more sodium must be supplied to sustain the corona and this sodium does not make it very far from Io.

Although the intercept is not a strong function of orbital phase for any of the three cases tested here, the steepness of the corona does show an orbital phase modulation which increases in magnitude as the torus electron density increases. This is another effect of the sodium lifetime differences between the three cases. When the electron densities are half the Voyager values, several things happen. First, the lifetime is long enough that more sodium with escape velocity does escape without being ionized. Second, the sodium that does not escape remains in the corona longer and mixes with sodium ejected from a range of orbital phases and magnetic longitudes, reducing the importance of Io's motion. The east/west electric field does still have an effect: the lifetime east of Jupiter is greater than the lifetime west of Jupiter. Therefore, the east/west brightness ratio is greater than one, although damped relative to the the nominal Voyager case. When the electron densities are twice the Voyager values, the orbital phase effect becomes much stronger because there is a larger range in the average lifetime experienced by each atom. Near western elongation, the lifetime is short and atoms are ionized very close to the source creating a steep corona. Near eastern elongation, atoms survive longer and travel farther before ionization creating a shallower corona.

Some of the observed variation in the slope of the corona can result from vari-

ations in the torus electron density. The slope was observed to vary between 2.0 and 2.6 (Chapter 3). Increasing the electron density by 2/3 over the nominal Voyager measurements decreases the sodium lifetime by a sufficient amount to produce a slope of 2.6. However, it is not possible to increase the sodium lifetime enough to create a slope as flat as 2.0 without also changing the initial speed distribution. If the electron density is decreased to zero (i.e., no sodium ionization), then the corona slope is 2.2 when  $v_p = 0.7 \text{ km s}^{-1}$ . This differs from the  $b^{-1}$  dependence of a freely escaping corona due to Io's gravitational force slowing the atoms. Therefore, decreases in torus density alone are not responsible for all of the observed variation in the corona.

The second change in the torus to examine are variations in the ion temperatures. The ion temperature controls the scale height of electrons which in turn affects the lifetime of sodium when Io is off the centrifugal equator. The scale height is proportional to the square root of the ion temperature: when the ion temperature is higher, the torus is “taller” and the range of electron densities is smaller. Therefore, the range of sodium lifetimes is smaller and there is less variability in the corona with magnetic longitude. In practice, the magnetic longitude effect is not very strong – there does not in fact appear to be any significant variation in the coronal density with magnetic longitude, even for the case where the ion temperature is half the Voyager value.

Changing the scale height does have a measurable effect, however (Figure 6.8). When the scale height is large, the electron density remains close to the equatorial value for all Io magnetic latitudes. Therefore the average lifetime is lower (i.e., the average lifetime is closer to the lifetime when Io crosses the centrifugal equator where it is minimized), and the corona is steeper. Shorter lifetime implies that less sodium makes it to the outer edges of the corona. The top three panels in Figure 6.8 show contours of sodium lifetime for ion temperatures equal to half to Voyager values, the Voyager values, and twice what Voyager measured. At magnetic longitudes near where Io crosses the centrifugal equator ( $\lambda_{Io} = 110^\circ$  and  $290^\circ$ ), the lifetimes do not change

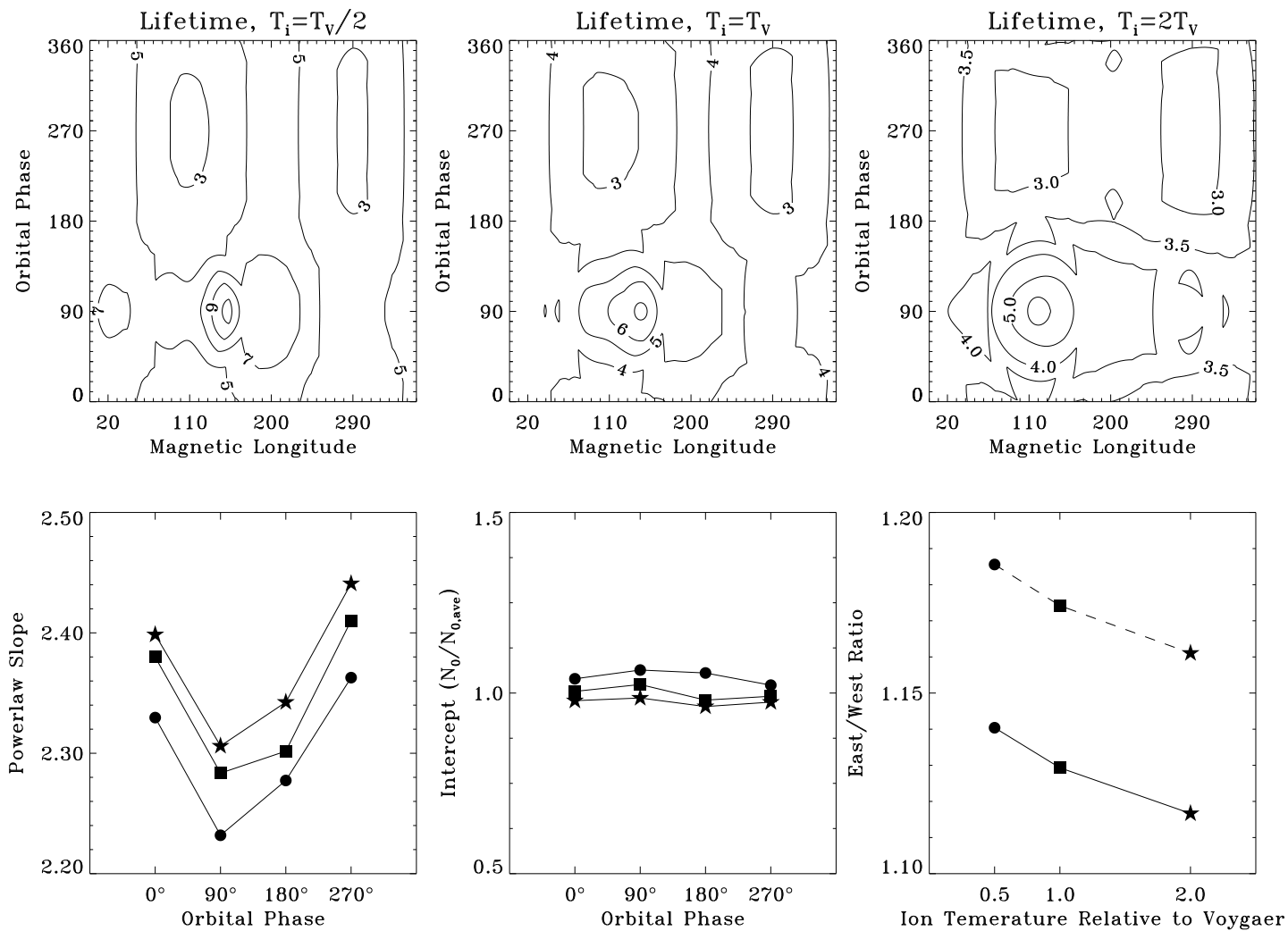


Figure 6.8 Effect of uniformly varying the ion temperature in the plasma torus on the sodium corona. Panels the same as in Figure 6.7 using the ion temperature equal to 1/2, 1, and 2 times the Voyager value. 129

between the three cases since the electron densities at the centrifugal equator do not depend on the ion temperature. The greatest changes occur when Io is at its greatest extent north or south of the torus ( $\lambda_{Io} = 200^\circ$  and  $20^\circ$ , respectively). Doubling the ion temperature results in the scale height varying by  $\sqrt{2}$ ; since electron density  $\sim e^{\zeta/H}$ , changes in the scale height affect the rate at which the electron density, and therefore the sodium lifetime, decreases off the centrifugal equator.

The shape of the corona is not strongly influenced by the changing ion temperatures. There is a trend, however, that can be discerned: as the ion temperature increases, both the slope increases and the intercept decreases. The reasons for this are similar to the reasons for the similar trends seen with increasing electron density discussed above: as the average sodium lifetime decreases, the corona is less extended and the number of atoms supplied to the corona must increase. The changes in each of these quantities are small, comparable to the observational limits of the mutual event observations. Changes in electron density have a much larger effect on the lifetime owing to the fact that the ion temperature variations only affect the lifetime of sodium off the centrifugal equator.

Changes in the ion temperature are not responsible for the observed variation in the slope of the corona: the ion temperature must be increased by an order of magnitude to create a corona as steep as observed. This increases the scale height by a factor of 3 which is large enough that the electron density only varies by 5% due to Io's motion off the centrifugal equator. Similarly, decreasing the scale height to zero, such that the electron density drops to zero immediately off the centrifugal equator, cannot produce a corona as shallow as that observed.

For the third test, I adjusted the strength of the east/west electric field using the parameter  $\epsilon$  ( $\epsilon$  is proportional to the strength of the electric field; see Section 5.3.2). The results from the case where the electric field is turned off or at its observed strength are shown in Figure 6.5; a comparison of these cases with that where the field strength is

doubled is given in Figure 6.9. The orbital phase variations of both the power law slope and intercept are strongly influenced by the strength of the electric field, consistent with the previously discussed conclusion that the east/west electric field is responsible for the east/west brightness asymmetry. Doubling the value of  $\epsilon$ , doubles the offset of the torus to the east and changes the regions of the torus seen by Io. In addition the local time modulation factor is proportional to  $(\epsilon/\epsilon_0)^2$ , so that both the torus shift and densities are affected and the orbital phase asymmetry becomes even more pronounced.

### 6.3.5 Effect of Magnetic Longitude Variations on the Corona

The scale height and electron density in the plasma torus have been observed to vary with magnetic longitude (summarized in Chapter 5). This variation is treated as a variation in the parallel ion temperature with  $\lambda_{III}$  according to Equation 5.11. The scale height and electron density vary as described in Equation 5.12 such that the total flux tube content along field lines remains constant as suggested by Schneider et al. (1997). The amplitude of this variation observed by Schneider and Trauger (1995) is  $0.5 \times T_0$  where  $T_0$  is the mean ion temperature. In this section I describe the effects of this variation on the shape of the corona.

The variation in corona shape versus System-III longitude is shown in Figure 6.10 for several amplitudes of variation. The model results are fit in the with equations in the form of:

$$y = y_0 + A \cos(2(\lambda - \lambda_0)) \quad (6.3)$$

where  $y$  is the power law slope, power law intercept, or the brightness through the Bergstrahl slit. Two wave cycles are fit over the full magnetic field rotation since the torus is symmetric along the field line above and below the centrifugal plane.

There are several important trends seen in these results. First, the magnitude of the variation in the shape of the corona increases with increasing amplitude of the System-III variation in the torus. Simply put, the greater the torus variability, the

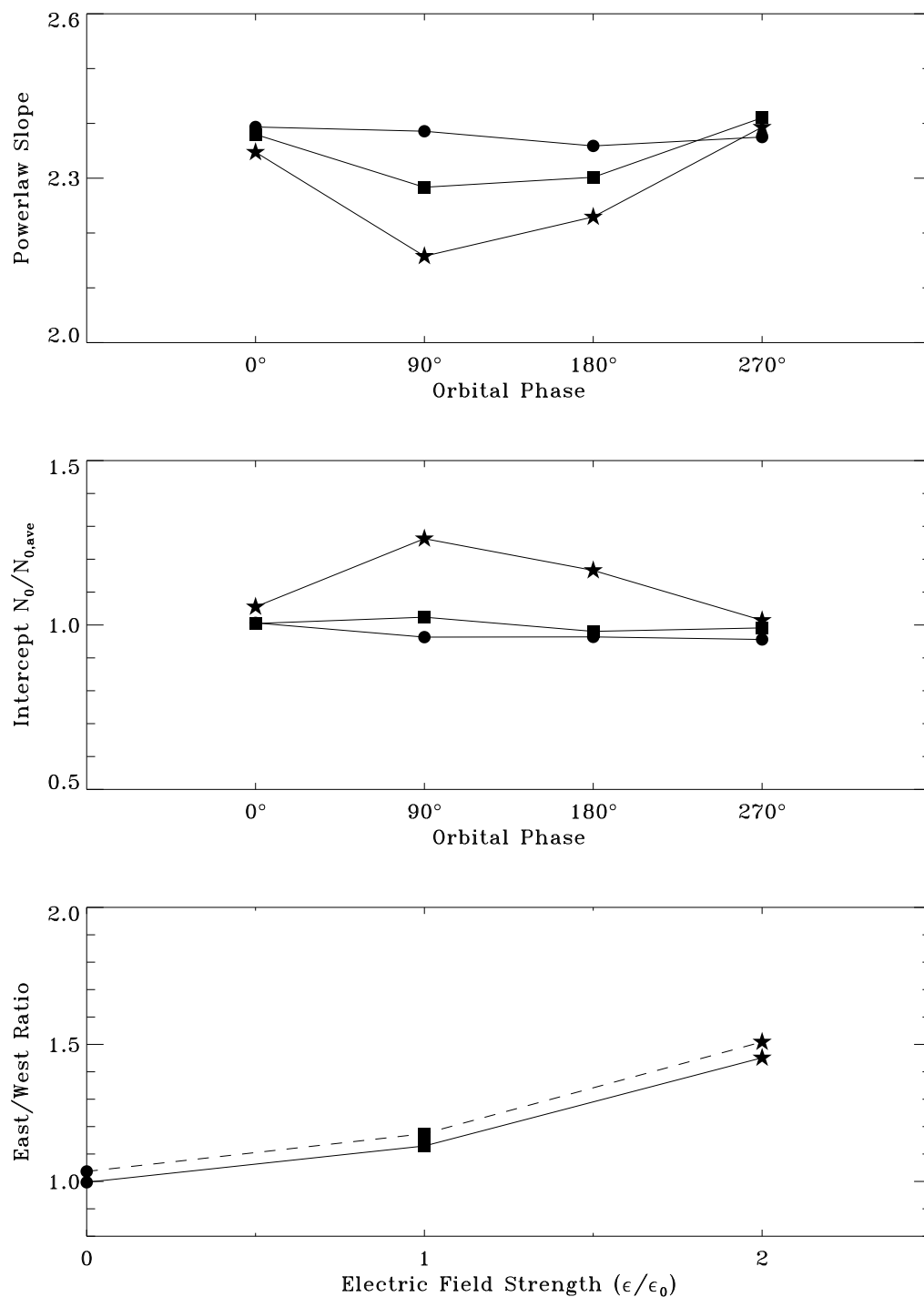


Figure 6.9 Effect of varying the strength of the east/west electric field on the sodium corona. The top panel shows the power law slope as a function of orbital phase; the middle panel shows the power law intercept; and the bottom panel shows the east/west column density ratio (solid line) and brightness ratio (broken line). The circles, squares, and stars represent the cases where  $\epsilon = 0, \epsilon_0$ , and  $2\epsilon_0$ , respectively, with  $\epsilon_0$  being the inferred value of  $\epsilon$ .

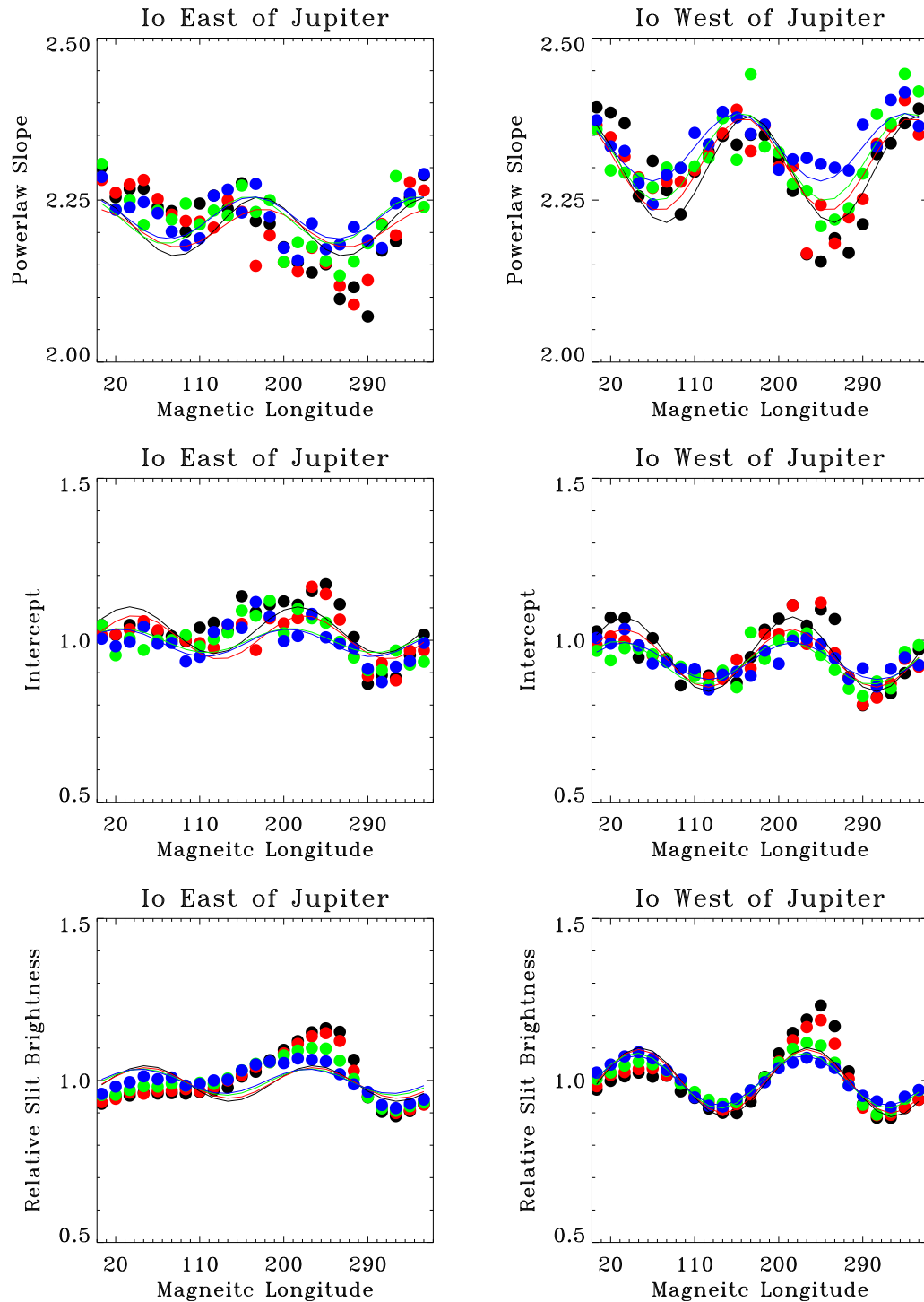


Figure 6.10 Effect of magnetic longitude variations in the plasma torus on the shape of the corona. The left panels show the corona when Io is east of Jupiter; the right panels are when Io is west of Jupiter. The top panels show the slope of the corona, the middle panels show the intercept, and the bottom panels show the relative brightness through the Bergstrahl slit. The amplitudes of the ion temperature variation relative to the mean ion temperature with  $\lambda_{III}$  are 0.0 (blue), 0.5 (green), 0.75 (red), and 0.9 (black). The lines show the sinusoidal fits discussed in the text.

greater the corona variability. There are two peaks in the slit brightness (bottom panels) for Io both east and west of Jupiter: one at  $\sim 50^\circ$  and the second at  $\sim 230^\circ$ . The longitudes of these peaks are determined by maximizing the sodium lifetime. This is a balance of two factors: (a) the greatest extent of Io from the centrifugal equator ( $\lambda_{Io} = 20^\circ$  and  $200^\circ$ ) and (b) the point of minimum torus scale height ( $\lambda_{III} = 226^\circ$ ). Looking at the case with no System-III variation (blue points), where only the first factor needs to be considered, shows that the peaks are delayed from Io’s maximum extent from the centrifugal equator by  $30^\circ$  to the point where the average lifetime experienced by the atoms is largest. As the amplitude of the torus variation increases, the height of the first brightness peak (at  $\lambda_{Io} = 50^\circ$ ) decreases and the height of the second peak (at  $\lambda_{Io} = 230^\circ$ ) increases. This happens because the sodium lifetime is increased over its previous maximum near the second peak and decreased near the first peak due to the varying scale height in the torus. The magnitude of this effect is small ( $\sim 5\%$ ), but observable with precise photometry over several hours when Io is near elongation.

#### 6.4 Understanding the Inner/Outer Asymmetry in the Corona

As shown in Chapter 3, there is an inner/outer asymmetry in the sodium corona: the inner (sub-Jupiter) hemisphere is consistently denser than the outer (anti-Jupiter) hemisphere. Both sides of the corona, however, drop off at approximately the same rate: i.e., the slopes on the inner and outer sides are the same, but the value of  $N_0$  over the outer hemisphere is approximately 0.6 times  $N_0$  over the inner hemisphere. In this section I discuss possible origins of this asymmetry. Because the regions measured are over the the sub-Jupiter and anti-Jupiter hemispheres, and the source regions are varied over the same hemispheres, I use the following nomenclature in this section: The terms “inner” and “outer” will refer to measurements over the sub-Jupiter and anti-Jupiter hemispheres, respectively. Uses of the terms “sub-Jupiter,” “anti-Jupiter,” “leading,” or “trailing” hemispheres refer to an exobase source confined to that region (Figure 6.11).

Models of the corona created with a source region which is uniform over Io's exobase in a torus that is roughly uniform across the corona are radially symmetric about Io. These are the conditions present for the models thus far discussed in this chapter. A spatially asymmetric corona therefore implies a non-uniformity in either the source or the sink.

To simulate this asymmetry, I divided the exobase into hemispheric regions such that the source could differ between each half of Io. The exobase was divided into either (a) the sub-Jupiter hemisphere (Io surface longitudes between  $270^\circ$  and  $90^\circ$ ) and the anti-Jupiter hemisphere (longitudes  $90^\circ$ – $270^\circ$ ), and (b) the leading (longitudes  $0^\circ$ – $180^\circ$ ) and trailing (longitudes  $180^\circ$ – $360^\circ$ ) hemispheres.

Figure 6.12 shows the shape of the corona when the sputtering is confined to either the sub-Jupiter, anti-Jupiter, leading, or trailing hemisphere. Each hemisphere individually can approximately supply the necessary ratio of escaping to non-escaping sodium to produce the observed corona profile over one side of Io, but not over both simultaneously. The slopes on each side are similar to the observed slopes, but the inner/outer ratio is not adequately modeled when the source is limited to a single hemisphere. Sputtering from the sub-Jupiter side primarily supplies sodium to the inner hemisphere and sputtering from the anti-Jupiter side primarily supplies sodium to the outer hemisphere. The leading and trailing hemispheres supply roughly equal amounts to the inner and outer hemispheres; if sputtering were limited to one of these regions, there would not be an observable inner/outer asymmetry.

Since a single hemisphere cannot supply the entire corona in the necessary ratio, I combine hemispheric sources to match the observations. Figure 6.13(a) shows the profiles in a corona formed by adding different proportions of the corona formed from a completely sub-Jupiter sputtering source and a completely anti-Jupiter sputtering source. The shape of the sputtering distribution from each hemisphere is the same; i.e.,

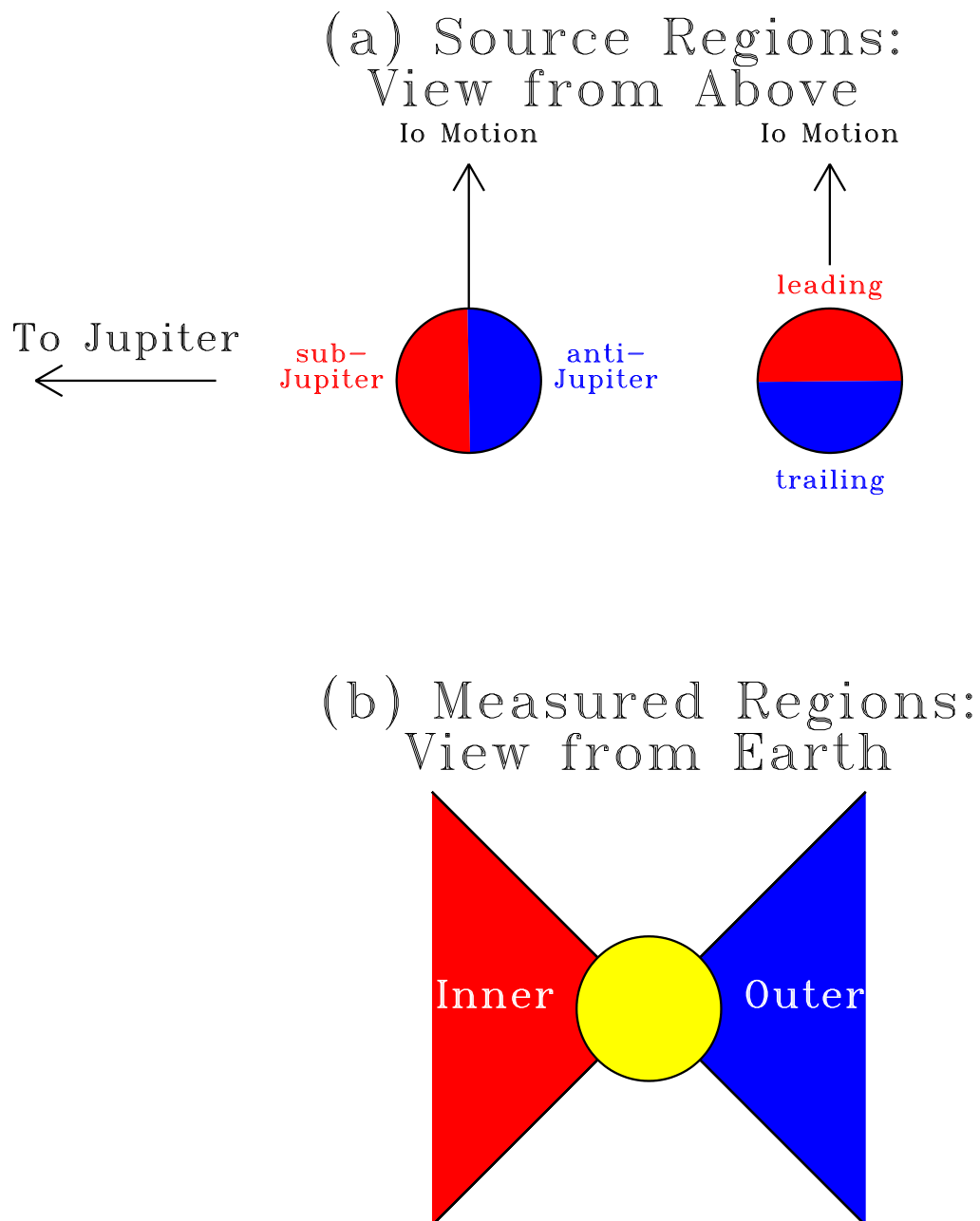


Figure 6.11 Sketch showing the nomenclature used for discussion of the asymmetry in Io's corona.

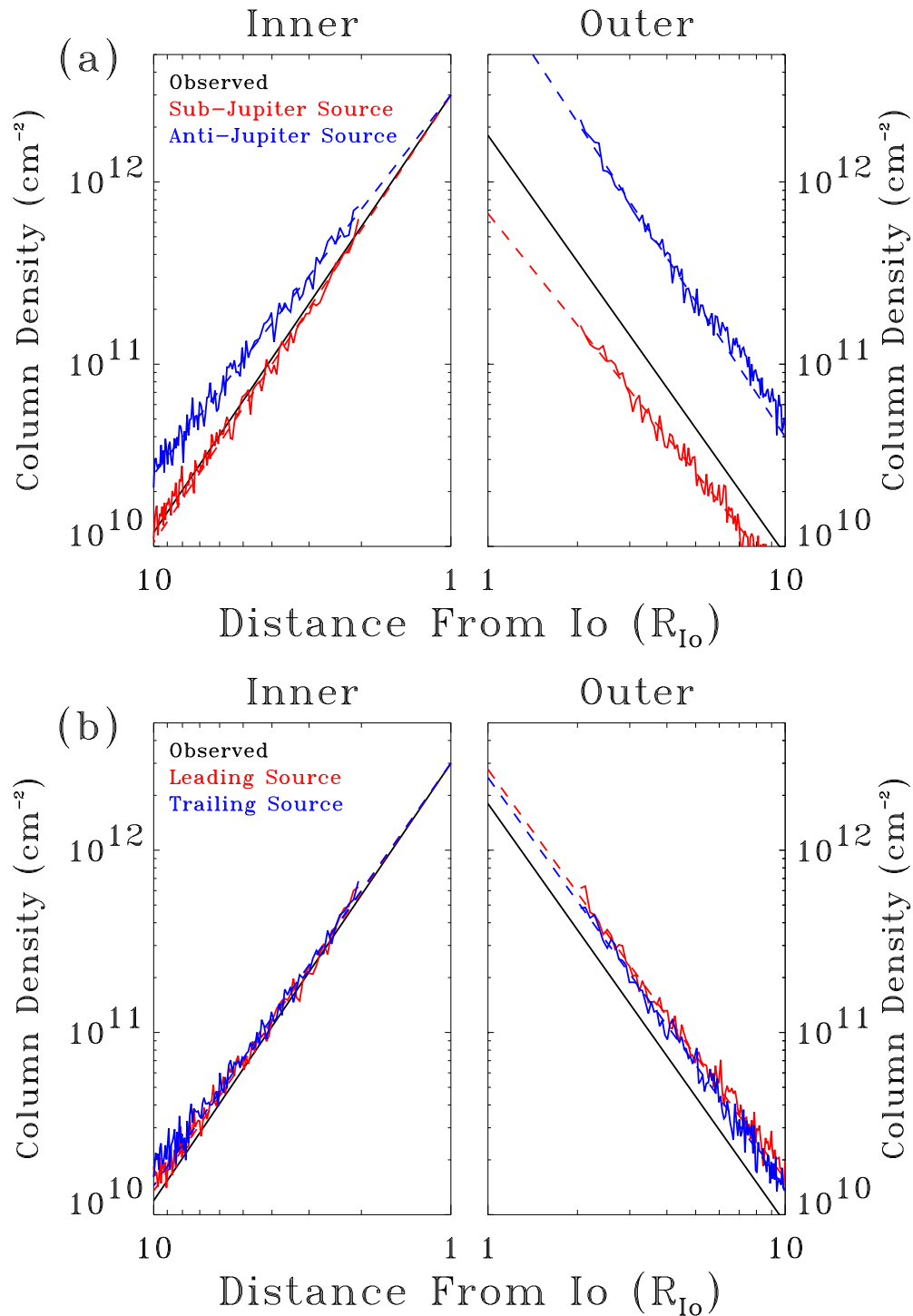


Figure 6.12 Shape of the corona when the source region is limited to a single hemisphere. The black lines in each panel are the observed asymmetric corona. In panel (a), the red lines show the simulated corona when sodium is only sputtered from the sub-Jupiter hemisphere scaled such that the inner modeled profile has the same  $N_0$  value as the inner observed profile. The blue lines represent the corona where the source is limited to the anti-Jupiter hemisphere, similarly scaled to the observed inner corona. The broken red and blue lines are the best fits to the red and blue model profiles extrapolated to the surface. Panel (b) shows the simulated coronae for sodium sources constrained to the leading hemisphere (red) and trailing hemisphere (blue).

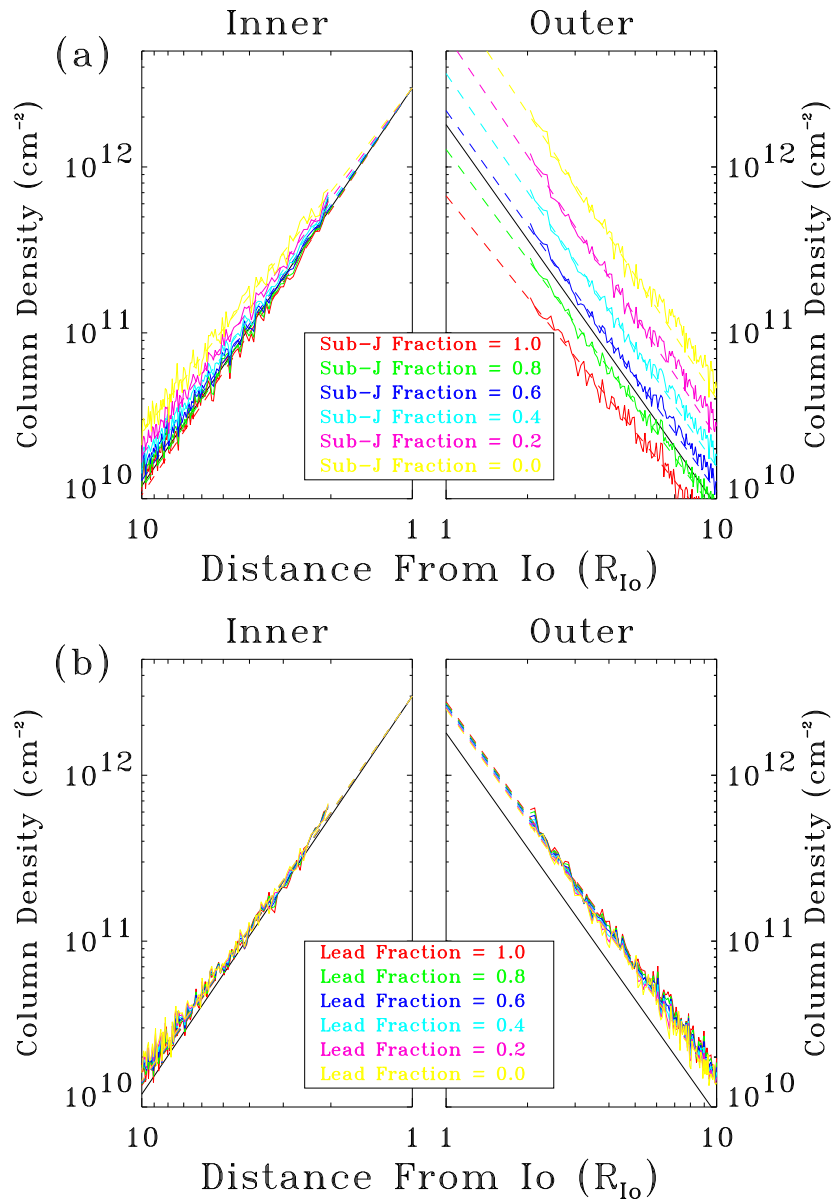


Figure 6.13 (a) Shape of the corona with sodium sputtered from the sub-Jupiter and anti-Jupiter hemispheres mixed. The colors show the fraction of the total source sputtered from each hemisphere. The modeled coronae are scaled such that the surface intercept on the inner hemisphere matches the observations (black lines). The broken colored lines show the fits to the modeled coronae extrapolated to the surface. (b) Shape of corona with sputtering from the leading and trailing hemispheres mixed.

each side has  $v_p = 0.7 \text{ km s}^{-1}$ . Figure 6.13(b) similarly combines sputtering from the leading and trailing hemispheres.

The first conclusion demonstrated in Figure 6.13 is that the observed corona asymmetry could be created by a sputtering source concentrated on the sub-Jupiter hemisphere: a source with 70% of the total sputtered sodium ejected from the sub-Jupiter hemisphere and 30% ejected from the anti-Jupiter hemisphere reproduces the observations. The observed asymmetry cannot be created by a leading/trailing source asymmetry. Since these hemispheres supply sodium to the inner and outer corona in equal proportions, asymmetric loss from these exobase regions does not create an inner/outer corona asymmetry. It would create a difference between the leading and trailing hemispheres, but no evidence for such an asymmetry was detected (but see below for a discussion of the observed oxygen corona asymmetry).

An inner/outer asymmetry would also be created if the most probable velocities on each side of Io were different. However, the characteristics of an asymmetry formed in this manner are different from that observed. Figure 6.14 shows the consequences of having half the sputtered sodium ejected from each hemisphere but allowing different sputtering distributions from the sub-Jupiter and anti-Jupiter hemispheres. The shape of the corona over one hemisphere is not significantly affected by the sputtering distribution on the opposite hemisphere. Changing the velocity distribution from the sub-Jupiter hemisphere does not affect the corona over the outer hemisphere, and vice-versa. The main effect is that the slope on the opposite side is more or less steep, depending on whether the velocity over that hemisphere is decreased or increased. The slope over a hemisphere is governed by the source distribution on that side; the opposite hemisphere provides sodium, but not enough to affect the shape of the profile. Therefore, the corona asymmetry can not be described simply as a difference in the shape of the sputtering distribution but instead must indicate a difference in the amount of sodium sputtered from each hemisphere. There may be a small difference in the shape

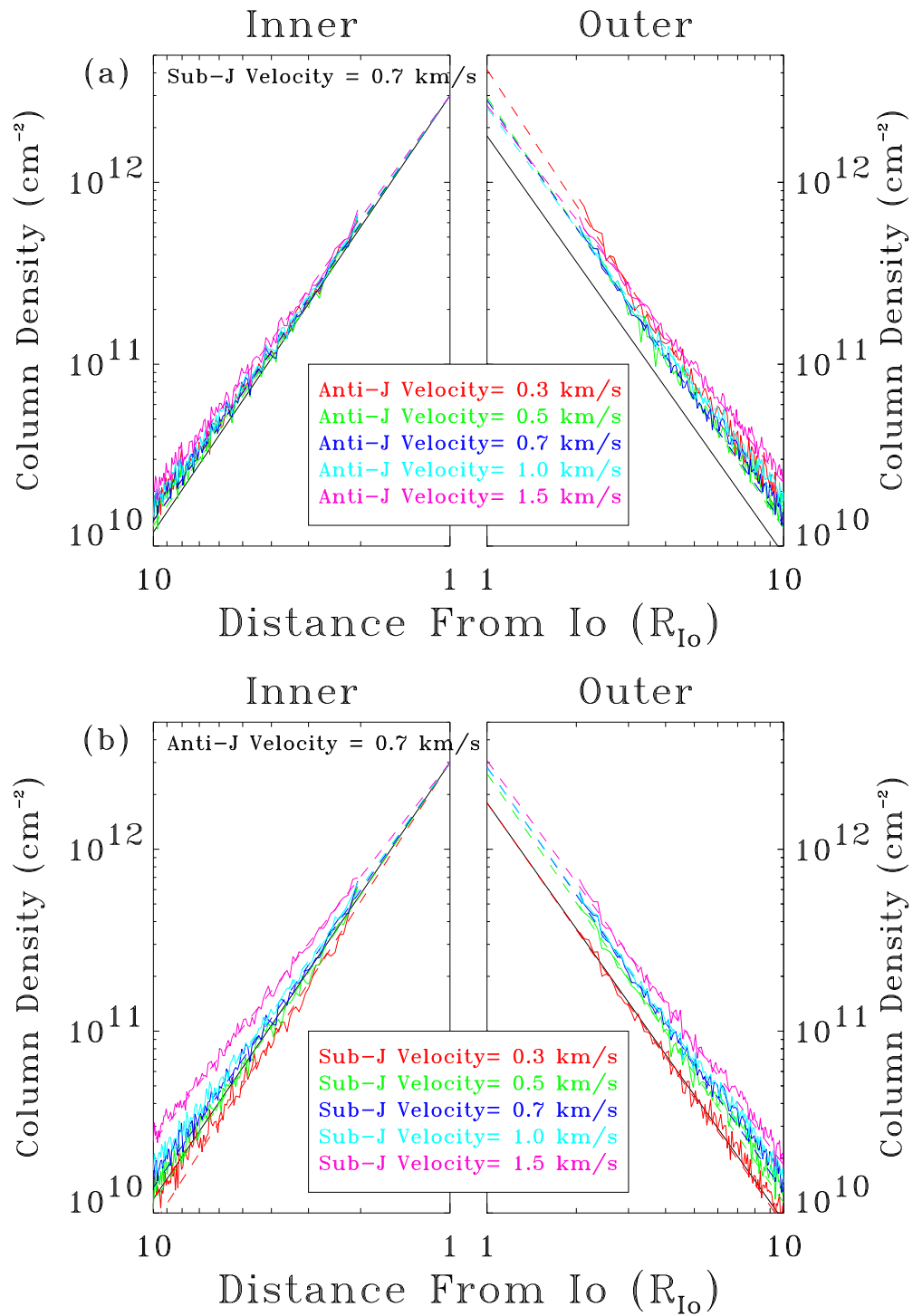


Figure 6.14 Shape of the corona when the most probable velocities of each hemisphere are allowed to vary independently. In panel (a), the velocity is held constant from the sub-Jupiter hemisphere ( $v_{\text{sub}} = 0.7 \text{ km s}^{-1}$ ) and allowed to vary from the anti-Jupiter from  $v_{\text{anti}} = 0.3 - 1.5 \text{ km s}^{-1}$ . Vice-versa for panel (b). Each hemisphere supplies half the sodium.

of the source distribution implied by the small observed difference in slope measured by the mutual events, but this difference is dominated by the different source rates.

One possible source of this sodium asymmetry is the effect of the electrodynamic interaction caused by Io moving through Jupiter's rapidly rotating magnetic field. Retherford et al. (2000) presented observations of equatorial spot emission near Io's surface. They found that the spot on Io's anti-Jupiter side was consistently brighter than the sub-Jupiter spot. The explanation for this lies in model results that the Io interaction deposits more energy on the anti-Jupiter side than the sub-Jupiter side (Saur et al. 2000). The additional energy is not enough to ionize oxygen, just to excite the emission. Sodium, however, has a lower ionization potential. Therefore energy which excites oxygen can ionize sodium. The equatorial spots are observed close to Io's surface implying that the interaction region is closer to Io than the regions probed by the mutual event observations. The increased sodium ionization would only occur in this region and would reduce the rate at which sodium is released into the corona.

Ionization near the exobase would also likely affect the velocity distribution of the atoms which do escape into the corona. Slower atoms, which spend more time in the interaction region would be preferentially ionized, increasing the most probable speed of the velocity distribution from the anti-Jupiter hemisphere. As seen in Figure 6.14(a), increasing the velocity from the anti-Jupiter hemisphere over that from the sub-Jupiter hemisphere corresponds with a small decrease in the slope from that hemisphere. This is consistent with the mutual event observations which suggested that there is a small difference in the measured slopes, although this difference was within the errors of the measurements.

## 6.5 Io's Oxygen Corona

Until recently, mutual events provided the only means of measuring the radial profiles of Io's corona. New techniques utilizing FUV observations of Io's emissions with

the *Hubble Space Telescope*, however, have made it possible to obtain spatially resolved images of Io's atmosphere and exosphere (Roesler et al. (1999), Figure 6.15). Besides the obvious advantage that the observations target the most abundant coronal species, the wavelengths observed are in the FUV where the solar continuum is negligible. Therefore the observations can be made any time Io is visible and it is not necessary to wait for the rare mutual events. The disadvantage of this method of observing the corona is that the emission intensity is a function of both the column density of oxygen and the state of the plasma. Therefore, complex modeling of the plasma interaction near Io is needed to truly understand the observations.

### 6.5.1 Observations

The data used by Wolven et al. (2001) consist of a series of spatially and spectral resolved images of Io's atmospheric and coronal emissions taken between 1997 and 2000. Images of Io's disk at discrete wavelengths are spread out with the wavelength increasing from left to right. Many of the images overlap due to the fact that bright transitions of several of the abundant species in Io's atmosphere and the plasma torus are similar in energy. However, several strong lines from the neutrals are uncontaminated allowing an unambiguous measurement of the intensity. In particular, Wolven et al. (2001) studied a semi-forbidden line of neutral oxygen at  $1356 \text{ \AA}$  and an allowed transition of neutral sulfur at  $1479 \text{ \AA}$ . The vertical direction on the detector records emission at constant wavelength. Therefore, Wolven et al. were able to determine the brightness profiles of oxygen and sulfur on opposite sides of Io. Unfortunately, due to the pointing constraints of *HST*, they were not able to align the slit at an arbitrary angle to Io's equatorial plane: the slit was aligned north-east to south-west relative to Jupiter's north pole for all the observations.

Two major differences were detected between the intensity profiles in the oxygen corona and sodium column density measurements. First, the oxygen intensity decreases

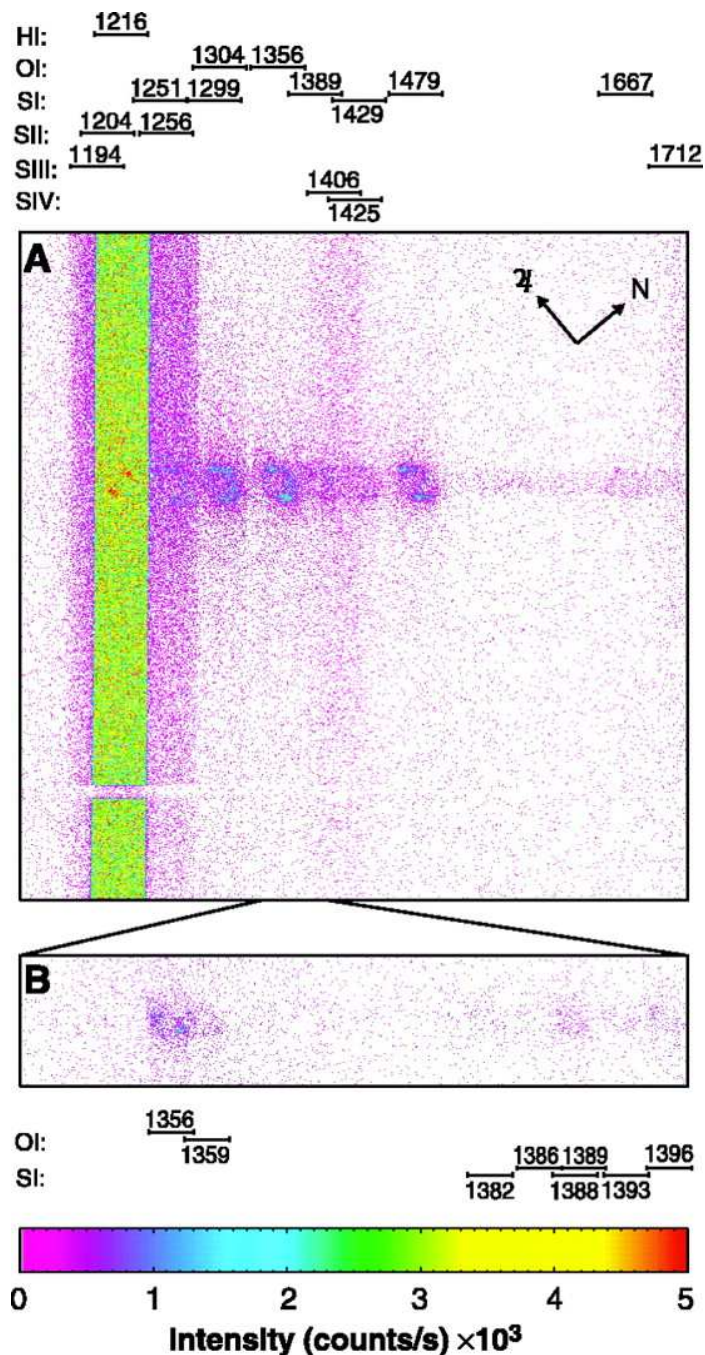


Figure 6.15 Example of STIS image of Io's atmospheric emissions. The circular features in a row just above mid-image are images of Iogenic emission at various O I and S I multiplets; faint, diffuse emission extends above and below the brighter circular features. The vertical green bar is an image of the 52-arc sec by 2-arc sec slit filled with diffuse terrestrial H I Lyman-alpha emission. Also present are several plasma torus lines (vertical bars brighter at the top than the bottom) and the shadow of a 0.5-arc sec fiducial bar in the slit (horizontal band near the bottom). The key above shows the slit positions for various emission wavelengths. The compass shows the directions of Jupiter (east) and jovian north. (From Roesler et al. (1999)).

Location	Measured Profile
Downstream, west:	$I \sim b^{-1.95}$
Upstream, west:	$I \sim b^{-1.76}$
Downstream, east:	$I \sim b^{-1.71}$
Upstream, east:	$I \sim b^{-1.51}$

Table 6.2 Summary of the intensity profiles in the oxygen corona observed by Wolven et al. (2001).

at a slower rate than the sodium. Second, Wolven et al. did not detect an inner/outer oxygen asymmetry. They did however measure a leading/trailing asymmetry: the emissions from the leading (downstream) side of Io were brighter than from the trailing (upstream) side. The following subsections discuss each of these differences and suggest possible reasons why oxygen and sodium do not behavior in the same manner.

### 6.5.2 The Average Oxygen Corona

The average oxygen profiles measured by Wolven et al. (2001) are summarized in Table 6.2 for the upstream and downstream hemispheres of Io when Io is both east and west of Jupiter. The upstream/downstream asymmetry is discussed in the following subsection. The oxygen corona is substantially flatter and more extended than the sodium corona, which had an average slope 2.3. They attribute the difference in power law slopes to the fact that oxygen has a much longer lifetime than Io.

To test this hypothesis, I have conducted model simulation of Io's oxygen corona (Figure 6.16) producing the average column density profiles. Due to the long oxygen lifetime, there are no variations in the column density with magnetic longitude: the average lifetime that the atoms experience is roughly constant. Because the emission is excited by electron-impacts, the oxygen intensity varies greatly as a function of magnetic longitude. This effect is discussed in greater detail in Chapter 7. Although the value of the intercept is a strong function of magnetic longitude, the slope is not. This is due to the fact the the torus densities and temperatures in this model are roughly constant

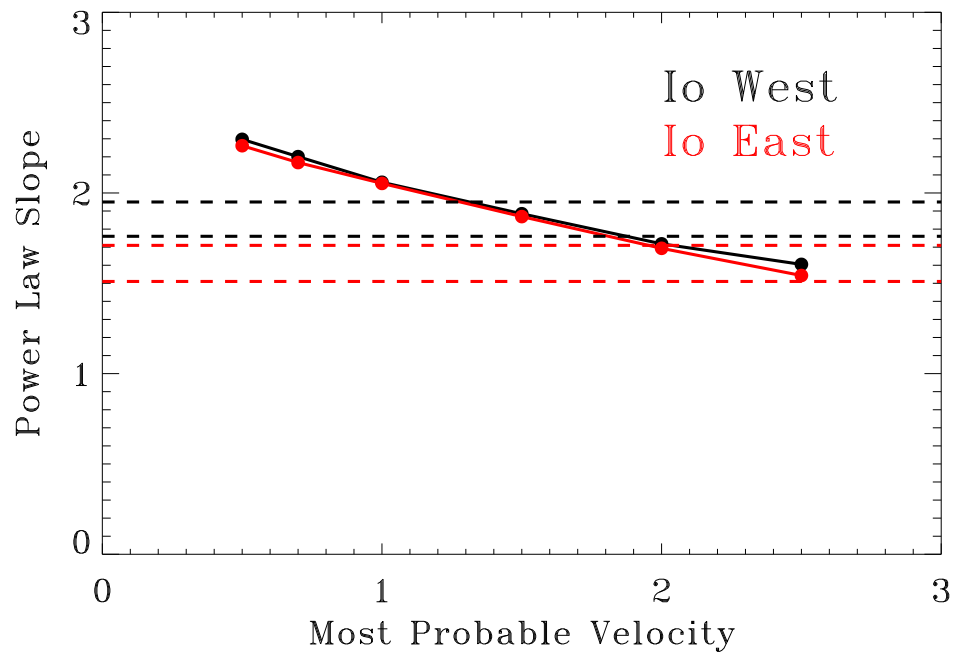


Figure 6.16 Power law slope in the oxygen corona as a function of the most probable speed of the sputtering distribution. The solid black line is the slope when Io is at western elongation; the solid red line is for Io at eastern elongation. The broken lines indicate the average upstream and downstream slopes observed by Wolven et al. (2001) and listed in Table 6.2

across the corona.

I conclude that the longer oxygen lifetime can only partly explain the difference between the shapes of the oxygen and sodium coronae. I found that the average sodium corona with a slope of 2.3 was well modeled with a classical sputtering distribution with a most probable speed of  $0.7 \text{ km s}^{-1}$ . An oxygen corona with this speed distribution would have a slope of 2.2, similar to the sodium corona although slightly more shallow. The increased lifetime does not have a large effect on the shape of the corona because the atoms which are escaping make it to the outer edge of the corona without much loss to ionization (Figure 6.17). Therefore, although the difference in lifetime is significant, lifetime alone cannot explain the observations.

A shallow oxygen corona would form if the oxygen were ejected from Io with a higher average speed than sodium. In Figure 6.16, the limits set by the average upstream and downstream slopes imply that the most probable speed of the sputtering distribution must be between  $1.4$  and  $2 \text{ km s}^{-1}$ . As discussed in Section 6.3, the shape of the corona can be modeled with an initial speed distribution other than the sputtering distribution. Dissociation of the most abundant species in Io's atmosphere,  $\text{SO}_2$ , into atomic oxygen and sulfur ( $\text{SO}_2 \rightarrow \text{O} + \text{SO}$ ,  $\text{SO} \rightarrow \text{O} + \text{S}$ ) might be an important source of neutrals in the corona. If the dissociation occurs near Io's exobase, the oxygen might be ejected fast enough to supply a large amount of oxygen to the outer edge of the corona and flatten the profile. It is also possible that there is an unobserved extended  $\text{SO}_2$  corona. Dissociation of these molecules far from Io would provide additional oxygen atoms at the edges of the corona and would also create a corona which is less steep than the sodium corona.

An alternative explanation is that the radial profile difference results from a difference in the plasma conditions rather than a difference in the neutral column density. The Voyager flybys detected a decrease in the torus electron temperature near Io (Sittler and Strobel 1987). This variation would result in an apparent flattening of the

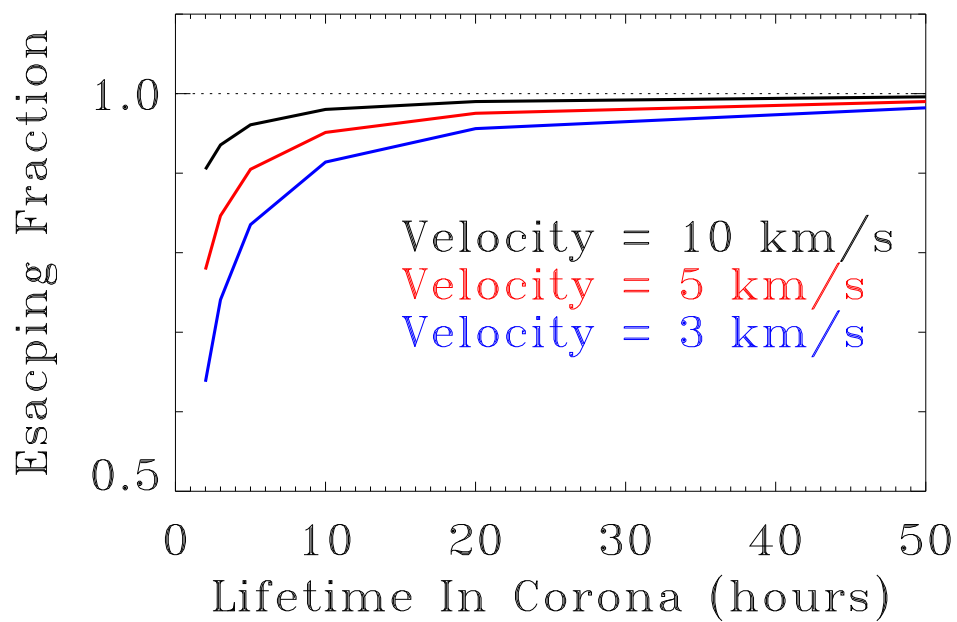


Figure 6.17 Fraction of atoms escaping from Io's corona as a function of neutral lifetime and initial velocity.

radial intensity profile in the corona (Figure 6.18). If the electron temperature near Io's surface is  $\sim 0.6$  the electron temperature  $10 R_{\text{Io}}$  from Io, then the modeled radial intensity profile matches the observations assuming that the oxygen is ejected from Io with the same sputtering distribution as sodium. The small dependence of the slope on  $T_e$  far from Io is due to non-linearities in the emission rate coefficient.

Wolven et al. noted that the slope of the oxygen corona when Io is east of Jupiter is shallower than when Io is west of Jupiter. Section 6.3.3 described the prediction that the sodium corona would show a east/west difference in slopes as an effect of the east/west electric field. This was shown to be the source of the east/west brightness asymmetry. The models of the oxygen corona however do not predict this asymmetry since any change in lifetime east to west is insignificant: as stated above, very little oxygen is ionized in the corona so changing the lifetime small amount does not have any effect. This difference can be explained by differences in the plasma torus at Io with the  $T_e$  decreasing more near Io at eastern elongation than at western elongation.

### 6.5.3 The Oxygen Asymmetry

Observations of both the sodium and oxygen coronae have detected asymmetries. However, the sodium asymmetry is a column density difference between the inner and outer hemispheres and the oxygen asymmetry is a brightness difference between the upstream and downstream hemispheres. The different natures of these asymmetries suggest that they are formed through different processes. In Section 6.4 I presented the hypothesis that the electrodynamic interaction as described by Saur et al. (2000) between Io and Jupiter's magnetic field decreases the sodium lifetime close to Io's exobase above the anti-Jupiter hemisphere and reduces the number of sodium atoms which can escape into the corona. Because the ionization potential of sodium is less than oxygen, the energy which excites the oxygen emission ionizes sodium. This creates a sodium asymmetry, but does not affect the ionization rate of oxygen resulting in a symmetric

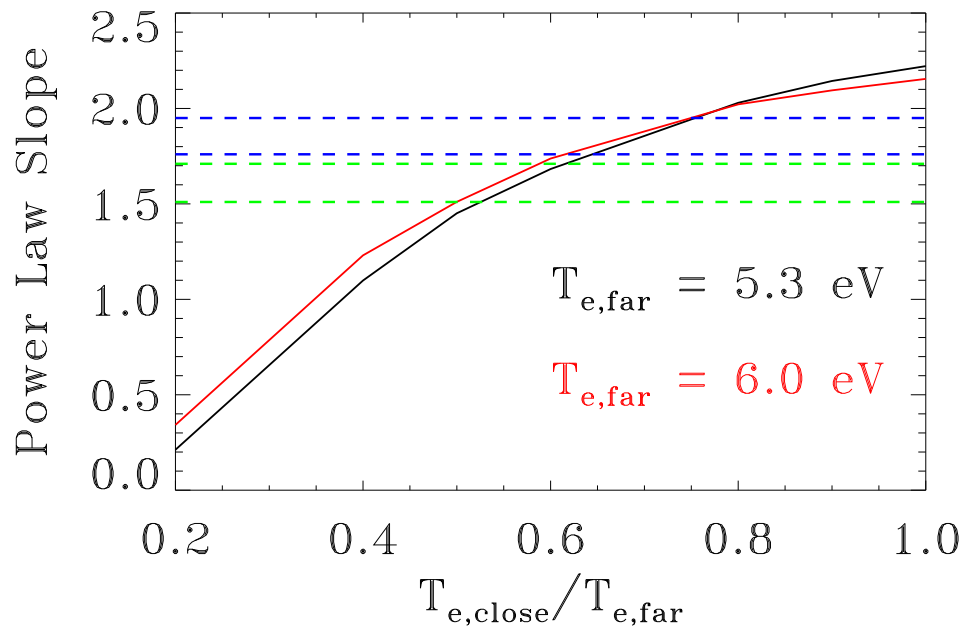


Figure 6.18 Power law slope of emission from the oxygen corona versus ratio of electron temperature at  $1 R_{Io}$  ( $T_{e,close}$ ) to electron temperature at  $10 R_{Io}$  ( $T_{e,far}$ ). The black line shows the slope for  $T_e=5.3 \text{ eV}$  at  $10 R_{Io}$ ; the red line shows the slope for  $T_{e,close}=6.0 \text{ eV}$ . The blue and green broken lines indicate the observed slopes by Wolven et al. (2001) for western and eastern elongations, respectively.

oxygen corona.

Wolven et al. (2001) attribute the asymmetry they detected to the increased electron density in Io's wake exciting greater emission from the downstream portion of the corona. Because my model of the plasma torus parameters does not include the interaction with Io, I am not able to address this question directly. The models of the sodium asymmetry described previously can be applied to understanding the ejection of neutral oxygen from Io's exobase assuming that the asymmetry is due to column density differences rather than differences in the emission rate. The sodium asymmetry was shown to result from greater sodium ejection from the sub-Jupiter hemisphere than the anti-Jupiter hemisphere. Ejection from either the leading or trailing hemisphere did not produce a difference in inner/outer column density asymmetry. Similarly, a difference between the ejection rates from the sub-Jupiter and anti-Jupiter hemispheres would not create an asymmetry between the downstream and upstream hemispheres. A column density asymmetry between these two regions implies that the source rate of oxygen from the leading hemisphere must be greater than from the trailing hemisphere.

## 6.6 Summary

The observations of the sodium corona presented in Chapter 3 have successfully been modeled using a classical sputtering source from Io's exobase. Atoms ejected isotropically with a most probable speed of  $0.7 \text{ km s}^{-1}$ , well below the escape speed from Io of  $2.1 \text{ km s}^{-1}$ , create a radially symmetric corona about Io which decreases in column density proportional to  $b^{-2.3}$ . The source rate of sodium necessary to match the observed column density is  $2.7 \text{ atoms s}^{-1}$ .

I then looked at deviations from the average corona starting with the effect of changing the source flux distribution function. The general trend holds that any change which increases the amount of high speed sodium that is ejected from the exobase creates a shallow, more extended corona. Decreasing the relative amount of sodium with escape

velocity results in a steeper corona which does not extend far from Io.

The state of the plasma in the plasma torus changes on short time scales. Even assuming there are no temporal or magnetic longitude variations in the plasma, Jupiter's rapid rotation rate combined with the offset, tilted dipole and the east/west electric field cause the plasma at Io to vary on rapid time scales. The different reasons for plasma variability at Io each have a different relative importance on the changing shape of the corona.

The most important factor shaping the observed corona is the east/west electric field. Jupiter's offset tilted dipole, without the electric field, does not create a corona which is much different from that which would be created with a torus that is not tilted relative to Jupiter's equatorial plane. This is because the lifetime variation induced by the dipole is too small to have a noticeable effect on ionization in the corona. The inclusion of the east/west electric field, by shifting the torus east more than  $0.1 R_J$  at Io's orbit, greatly increases the average lifetime at Io and the range of lifetime experienced by sodium in the corona. The sodium lifetime when Io is east of Jupiter is significantly longer than when Io is west of Jupiter, resulting in a shallower slope to the sodium column density profile east of Jupiter. The increase in slope corresponds with an increase in the total sodium abundance in the corona and therefore Io's sodium emissions are brighter when Io is at eastern elongation than at western elongation. Because the strength of the electric field affects both the slope and the overall column density, the east/west brightness ratio can be used as a probe of electric field strength.

Uniform variations in the electron density also change the shape of the corona. The sodium lifetime is inversely proportional to the electron density. The general trend is that the longer the sodium lifetime, the flatter and more extended the corona. Therefore, increasing the electron density creates a steep corona which remains close to Io. Decreasing the electron density forms a more shallow corona, but the slope only decreases to a point. Without the influence of Io's gravity, neutrals escaping without ion-

ization would have a column density profile proportional to  $b^{-1}$ . Io's gravity increases the slope such that for the average modeled flux distribution with  $v_p = 0.7 \text{ km s}^{-1}$ , the slope with infinite lifetime is  $\sim 2.2$ . To form a more shallow corona, it is necessary to reduce the importance of gravity by increasing the most probable speed of the escaping neutrals.

Changes in the ion temperature only affect the scale height in the corona and therefore do not have as large an effect on the corona as factors which affect the torus at all magnetic longitudes. The main effect is to reduce the System-III variability in the corona, although this variability is not very strong to begin with. Therefore it would be difficult to detect ion temperature variations in the torus by studying the corona. An additional effect of ion temperature increases is that the average lifetime in the corona is slightly longer due to the fact that there is a smaller departure from the maximum electron density. Therefore, the steepness of the corona is a weak function of the ion temperature.

Magnetic longitude variations in the torus have an effect on the coronal shape best seen by looking at the total sodium column through the corona. The brightness modulation is a double peaked function of magnetic longitude. The ratio of the brightnesses of these peaks is a function of the amplitude of the magnetic longitude variations. This a result of the fact that the tilt of torus causes a double peaked variation in the electron density which is modulated by the single peaked magnetic longitude variation. The magnitude of this effect is small, but should be detectable.

The observed inner/outer asymmetry most likely results from asymmetric loss from Io. The effective source rate from the sub-Jupiter hemisphere must account for 70% of the total sodium source. A possible mechanism for creating asymmetric loss from Io's exobase (i.e., an asymmetric coronal source), is an increase in the ionization rate close to the exobase from the interaction between Io and Jupiter's magnetic field. The interaction region is closer to Io than that measured by the mutual events. Increasing

the ionization rate reduces the supply rate of neutral sodium to the outer hemisphere creating the observed asymmetry.

The oxygen and sodium coronae have distinct morphological differences. Both the radially averaged slopes and the nature of their asymmetries are different. The different slopes cannot be explained by the difference in neutral lifetimes between the two species. If the difference in slopes is due to density differences, the shallower oxygen corona implies that the most probable speed of oxygen must be greater than sodium. Assuming a sputtering distribution, the most probable speed must be  $\sim 1.4 - 2 \text{ km s}^{-1}$ . However, dissociation of  $\text{SO}_2$ , a source mechanism available to oxygen but not sodium, could supply faster oxygen near the exobase or resupply the corona farther out. The difference in slopes could also be a result of the fact that oxygen intensity, rather than column density, was observed. An increase in electron temperature with increasing distance from Io, as observed by Voyager, decreases the slope of the radial intensity profile of oxygen.

The mechanism proposed for the sodium asymmetry does not create an inner/outer oxygen column density asymmetry; it does create an asymmetry in the oxygen emission close to Io's surface but not in the corona. The downstream/upstream asymmetry may result from increased electron density in the plasma torus wake (Wolven et al. 2001) or could imply a leading/trailing asymmetry in the oxygen source rates from the exobase. Due to the complex nature of the Io interaction and the strong dependence on the instantaneous state of the plasma on the emission rate it is not possible to distinguish between an emission rate asymmetry and a column density asymmetry.